A Doctoral Dissertation

Anticancer effect and cell death mechanism of phytochemicals in human gastric cancer cell lines

Department of Biotechnology

GRADUATE SCHOOL
JEJU NATIONAL UNIVERSITY

Jeong Yong Moon

February 2013

위암 세포주에서의 phytochemical에 대한 항암 효능 탐색 및 세포 죽음에 대한 기전 연구

지도교수 김소미

문정용

이 논문을 이학 박사학위 논문으로 제출함

2013년 2월

문정용의 이학 박사학위 논문을 인준함

심사위원장 鄭 基 中

부 위 원 장 趙 文 鎭

위 원 李 康 基

위 원 崔 京 均

위 원 金 昭 美

제주대학교 대학원

2013년 2월

Anticancer effect and cell death mechanism of phytochemicals in human gastric cancer cell lines

Jeong Yong Moon

(Supervised by Professor Somi Kim. Cho)

A thesis submitted in partial fulfillment of the requirement for the degree of doctor of philosophy in biotechnology

Date Approved :

Dec. 2012

Kyung Rim

Hyung-Kyoon Choi

Department of Biotechnology

GRADUATE SCHOOL

JEJU NATIONAL UNIVERSITY

February 2013

CONTENTS

List of Tables

List of Figures

List of Abbreviations

2D	2-dimensional
DMEM	Dulbecco's modified Eagle's medium
DMSO	Dimethyl sulfoxide
EOs	Essential Oils
FBS	Fetal bovine serum
MTT	3-(4,5-dimethyl-2-yl)-2,5-diphenyltetrazolium bromide
PBS	Phosphate buffered saline
PI	Propidium Iodide
SCEs	Supercritical Extracts
SDS-PAGE	Sodium dodecyl sulfate polyacrylamide gel electropheresis

PART I

INTODUCTION

1. Traditional *Citrus* sp. (dangyuja, phalsak, and yeagam) in Jeju

Citrus is one of the important fruits of high medicinal value and have long been the basis of commonly used traditional medicines in several Asian countries (Kubo *et al*., 2005). In addition to use as medicine source, citrus fruits are also widely used in cuisine materials as salad dressing, sauces, jams and vinegar as well as whole fresh fruits. The medicinal and commercial importance of these products leads to extensive scientific study resulting in a broad base knowledge of their chemical composition and bioactivities. Accumulated evidence from experimental and epidemiological studies indicates that dietary consumption of citrus fruit or juice appears to be inversely associated with lower risk of many infectious diseases including cancers (Benavente-Garcia and Castillo, 2008; Jayaprakasha *et al*., 2008**;** Huang *et al*., 2009). *Citrus grandis* Osbeck, *Citrus hassaku* Hort ex Tanaka and *Citrus iyo* Hort. ex Tanaka are locally known as “dangyuja”, “phalsak”, and “yeagam”, in Korea, respectively. These species are variably distributed in southeastern Asia, and the main areas of production are southern China, southern Japan, Thailand, Vietnam, Malaysia, and Indonesia. In some Asian cultures, the decoction of the fruit peel has been used for medicinal purposes to alleviate coughs, ulcers, swellings, and epilepsy, and the oil has a potential antiobesity activity (Hariya, 2003). Numerous investigations have shown the biological activities and chemical qualities of the essential oils from these species (Tsai *et al*., 2007; Mokbel and Hashinaga, 2006). The concentration of phytochemicals in plants depends on many factors, such as the cultivar type, growing conditions, and country of origin. Recently, a great deal of interest has expressed on the study of anticancer and antioxidant activities and characterize responsible phytochemical profiles in *Citrus* sp. (Lim *et al*., 2006; Yang *et al*., 2008). Furthermore, recent investigations from our laboratory have provided evidences for the health-promoting properties of citrus in cell culture studies, such as antioxidant

activity and prevention of cancer (Lim *et al*., 2009; Kim *et al*., 2010; Cho *et al*., 2009a; Moon *et al*., 2009).

2. Phytochemicals

Phytochemicals are non-nutritive plant chemicals that have protective or disease preventive properties. They are non-essential nutrients, meaning that they are not required by the human body for sustaining life. It is well-known that plant produces these chemicals to protect them but recent research demonstrates that they can also protect humans against some chronic diseases. There are more than thousand known phytochemicals. Some of the well-known phytochemicals are lycopene in tomatoes, isoflavones in soy and flavanoids in fruits (Arts *et al*., 2005).

There are various types of phytochemicals and each works differently. Most of phytochemicals have antioxidant activity and protect our cells against oxidative damage and reduce the risk of developing certain types of cancers. Phytochemicals with antioxidant activity: allyl sulfides (onions, leeks, garlic), carotenoids (fruits, carrots), flavonoids (fruits, vegetables), polyphenols (tea, grapes), etc. Isoflavones, found in soy, imitate human estrogens and help to reduce menopausal symptoms and osteoporosis. Indoles, which are found in cabbages, stimulate enzymes that make the estrogen less effective and could reduce the risk of breast cancer. Other phytochemicals, which interfere enzymes, are protease inhibitors (soy and beans), terpenes (*Citrus* fruits and cherries). The phytochemical, allicin from garlic has antibacterial properties. Some phytochemicals bind physically to cell walls thereby preventing the adhesion of pathogens to human cell walls. Proanthocyanidins are responsible for the antiadhesion properties of cranberry. Consumption of cranberries will reduce the risk of urinary tract infections and will improve dental health.

3. Gastric cancer

Gastric cancer is one of the most prevalent tumor types and the leading cause of cancer-related death in East Asia and Eastern Europe (Leung *et al*., 2008). Chemotherapeutic drugs commonly used in gastric cancer treatment are 5-fluorouracil (5-FU), cisplatin, and adriamycin (Ohtsu, 2008). Currently, chemotherapy regimens represent the primary treatment option for patients with gastric cancer (Wagner *et al*., 2006). However, a major obstacle in the successful treatment of gastric cancer is the resistance of gastric cancer cells to current chemotherapy and cell toxicity (Benson, 2006.). At the same time, cancer researchers have been intrigued by the ability of some natural products both to enhance the anticancer effects of therapy and to reduce side effects (El-Shemy *et al*., 2007). Hence, natural anticancer compounds that circumvent issues of drug resistance, toxicity, and side effects in the treatment of gastric cancer are greatly needed (Park and Lenz, 2006).

4. Apoptosis

In 1972, the term ‘‘apoptosis’’ was used for the first time to describe a form of cell death associated with specific morphological features. Since then, apoptosis has been extensively studied and underlying signaling events are now well characterized. Morphologically, apoptosis is associated with cell shrinkage, membrane blebbing, and chromatin condensation. It is a cell-intrinsic programmed suicide mechanism that results in the controlled breakdown of the cell into apoptotic bodies, which are subsequently recognized and engulfed by surrounding cells and phagocytes. Two main evolutionarily conserved protein families are involved in apoptosis, namely the Bcl-2 family of proteins, which control mitochondrial integrity (Youle and Strasser,

2008), and the cysteinyl aspartate-specific proteases or caspases, which mediate the execution phase of apoptosis (Fuentes-Prior and Salvesen, 2004).

5. Autophagy

Autophagy is an evolutionarily conserved catabolic pathway that allows eukaryotes to degrade and recycle cellular components. Proteins and organelles are sequestered in specialized double-membrane vesicles, designated autophagosomes, which are typical of autophagic cells. Basal levels of autophagy ensure the maintenance of intracellular homeostasis, but in addition, many studies have revealed its diverse functions in important cellular processes, such as cellular stress, differentiation, development, longevity and immune defense. Although a pro-survival role for autophagy is well established, frequently debated is whether or not autophagy has a causative role in cell death. The presence of autophagic vacuoles in dying cells has led to the introduction of autophagic cell death, although autophagy often accompanies rather than causes cell death. It is plausible though that massive autophagic activity could result in cellular demise. In addition, several interconnections exist between autophagy and apoptotic or necrotic cell death (Maiuri *et al*., 2007).

6. Scope of the study

The purpose of this study is the component analysis of three kinds of Jeju traditional Citrus (dangyuja, phalsak, yeagam) according to the method of extraction and its derived phytochemicals of antitumor activity for gastric cancer cells, and our results can be attributed to the research about the mechanism of cell death in gastric cancer cell lines.

PART II

Essential Oils of Jeju traditional *Citrus*

1. **Antiproliferative activity of Essential Oils**
2. **Antiproliferative activities of major compounds of Essential Oils**

1. ABSTRACT

Citrus essential oils (EOs) contain different types of terpens that have been shown to possess antitumor effects. We determined the cytotoxic effect of essential oils from *Citrus* peels in a gastric cancer cell line. The fruits selected for the extraction were of three types: *Citrus grandis* Osbeck (dangyuja), *Citrus hassaku* Hort ex Tanaka (phalsak) and *Citrus iyo* Hort. ex Tanaka (yeagam) from the harvest in the Jeju Island. EOs were extracted by hydrodistillation and analyzed by GC-MS. EOs content of Limonene was 86.41-64.69 % while α-Pinene and β-Myrcene were 1.8-0.49% and 32.23-2.02% respectively. Various concentrations of EOs (12.5-100 μg/mL) were added to cultured cells and incubated for 12, 24 and 48 h. Cell viability was evaluated using the MTT-based cytotoxicity assay. The IC_{50} value was more sensitivity to all EOs in AGS than SNU-1 and SNU-16. In conclusion, Jeju *Citrus* peels EOs obviously reduced the cell viability and it might have cytotoxic effect against gastric cancer cell line. In addition, we determine to effect of dl-Limonene, α-Pinene and β-Myrcene in gastric cancer cell lines. dl-Limonen reduced the viability of all type of gastric cancer cells. AGS was slightly reduced cell viability whereas, α-Pinene, and β-Myrcene dose not cytotoxic effect against SNU-1 and SNU-16.

2. INTRODUCTION

An essential oil is a concentrated hydrophobic liquid containing volatile aroma compounds from plants. Essential oils are also known as volatile oils, ethereal oils or aetherolea. Essential oils are generally extracted by distillation and steam distillation is often used. Other processes include expression or solvent extraction. They are used in perfumes, cosmetics, soaps and other products, for flavoring food and drink, and for adding scents to incense and household cleaning products. Various essential oils have been used medicinally at different periods in history. Medical applications proposed by those who sell medicinal oils range from skin treatments to remedies for cancer, and often are based solely on historical accounts of use of essential oils for these purposes. Claims for the efficacy of medical treatments and treatment of cancers in particular, are now subjected to regulation in most of countries. Several studies indicated that EOs have antitumor effects, monoterpenes have been reported to have a chemopreventive effect against rodent mammary, skin, liver, lung and fore-stomach cancers (Crowell, 1999). EOs from *Citrus* plants contain a high percentage of monoterpene hydrocarbons (70-95%) along with smaller amounts of sesquiterpene hydrocarbons, oxygenated derivatives and aromatic hydrocarbons (Mohamed *et al*., 2010; Siddique *et al*., 2011). *Citrus* oil mainly consists of limonene, α-Pinene, β-pinene, β-Myrcene and linalool (Siddique *et al*., 2011; Lota *et al*., 2001). Despite the many publications studying the compositions of *Citrus* peels EOs, no report on its cytotoxic effect is yet available. In this study, the composition of Jeju *Citrus* (*Citrus grandis* Osbeck, *Citrus hassaku* Hort ex Tanaka and *Citrus iyo* Hort. ex Tanaka) peels EOs was determined, and their cytotoxic effect against gastric cancer cell line was studied.

3. MATERIALS AND METHODS

3. 1. Reagents

dangyuja, phalsak, yeagam were obtained from (e-Jeju Agricultural Union Corporation) in the Jeju Province, Korea. RPMI 1640 medium, F12K medium, trypsin/EDTA, fetal bovine serum (FBS), penicillin, streptomycin, Hoechst 33342 dye, and Trizol were purchased from Invitrogen Life Technologies Inc. (Grand Island, NY, USA). Dimethyl sulfoxide (DMSO), MTT, PI, RNase A, and caspase activity assay kits were purchased from Sigma Chemical Co. (St. Louis, MO, USA).

3. 2. Preparation of the *Citrus* Essential Oils

EOs was extracted from fresh peels (100 g) collected by hydrodistillation for 3 h using a Clevenger-type apparatus. The oils were stored at -20°C for subsequent analysis.

3. 3. Cell culture

Gastric cancer (AGS, SNU-1, SNU-16) cells were maintained at 37ºC in a humidified atmosphere under 5% CO_2 in F12K or RPMI 1640 containing 10% heat-inactivated FBS, 100 U/mL penicillin, and 100 μg/mL streptomycin. Exponentially grown cells were treated with various concentrations of the solvent fractions, as indicated.

3. 4. Cell viability assay

The effect of the *Citrus* peels Essential Oils on the viability of various cancer cell lines was determined by a MTT-based assay. Briefly, exponential-phase cells were collected and transferred to a microtiter plate. The cells were then incubated in the presence of various concentrations of the *Citrus* peels EOs. After incubation, 5

mg/mL of MTT solution (Sigma, MO, USA) was added to each well and the cells were incubated at 37℃ for 4 h. Medium was carefully removed and then DMSO (150 μL) was added to each well to dissolve the formazan crystals. The plates were read immediately at 570 nm on a Sunrise microplate reader (Sunrise, Tecan, Salzburg, Austria). The concentration at which growth was inhibited by 50% (the IC_{50} value) was determined in triplicate for each well.

3. 5. GC-MS analysis

Chromatographic analysis was carried out using a Shimadzu GC-MS (model QP-2010, Shimadzu Co., Kyoto, Japan) attached to AOC-5000 autosampler in electron impact mode. The ionization voltage was 70 eV, and the temperatures of the injector and interface were 250^{o}C and 280^{o}C respectively. The capillary column used was an Rtx-5MS (30 m length, 0.25 mm internal diameter, and 0.25 μm film thickness). The oven temperature was programmed at 40^{o}C and was ramped to 200^{o}C at 3^{o}C/min and to 250^{o}C at 5^{o}C/min. Helium was used as the carrier gas at a flow rate of 1 mL/min with 57.4 kPa pressures, and an injector volume of 1 μL. Mass range was from m/z 40–500 amu. The extracts of the fruits were solubilized in n-hexane, filtered through a 0.20-μm syringe filter (Advantec, Tokyo, Japan), and aliquots were injected into the GC-MS. Mass spectra of each compound were tentatively identified with the mass spectral data contained within the WILEY7 and NIST05 libraries and by their Kovats indices relative to C_7–C_{30} n-alkanes (Sigma-Aldrich Chemie GmbH, Steinheim, Germany) on an Rtx-5MS column. Further tentative identification was completed by comparing the mass spectra with those of authentic standards (Adams, 1989).

4. RESULTS

4. 1. Cytotoxic effect of EOs

The effects of various concentrations of the dangyuja, phalsak, yeagam (*Citrus grandis* Osbeck, *Citrus hassaku* Hort ex Tanaka and *Citrus iyo* Hort. ex Tanaka) peels essential oils on the growth of gastric cancer cells were examined by the MTT-based assay (Fig. 1, 2, and 3). Among the cells tested, all EOs appeared to have similar antiproliferaive effect and the most potent effect in AGS. IC_{50} values were 14.83, 9.88, and 11.53 in danyuja, phalsak, and yeagam, in EOs-treated AGS cell for 12 h respectively (Fig. 1A, 2A, and 3A), while other cell lines (SNU-1 and SNU-16) IC_{50} values were about > 20 μg/mL.

A

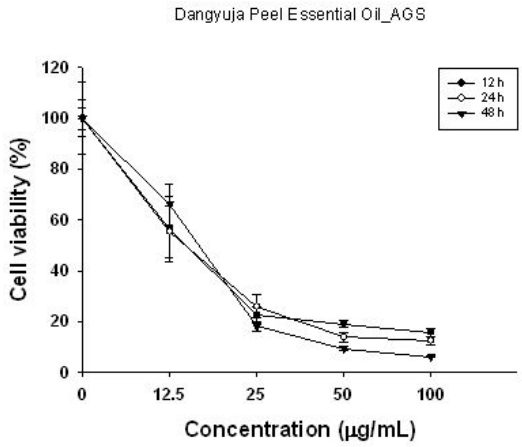

B

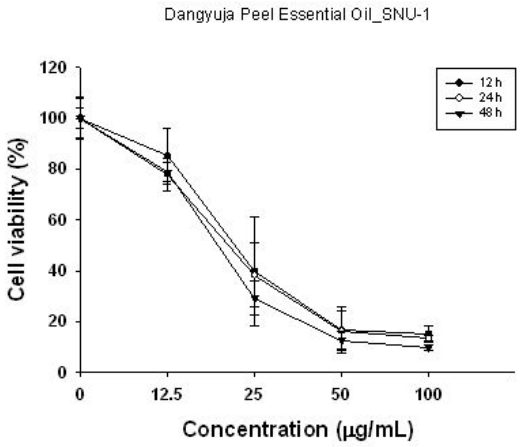

C

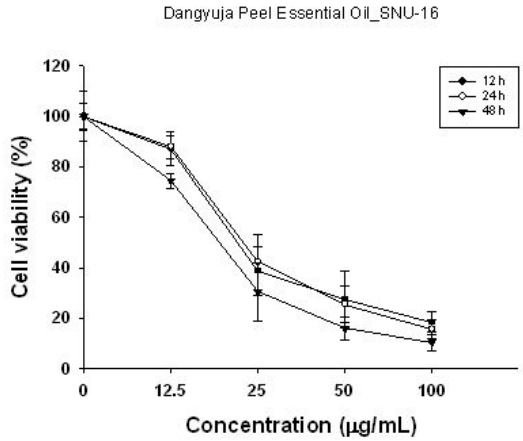

Figure. 1. Effect of the essential oil of dangyuja (*Citrus grandis* Osbeck) peel on cell viability after 12, 24, and 48 h. (A) AGS, (B) SNU-1, (C) SNU-16. Untreated (DMSO alone) cells were used as controls.

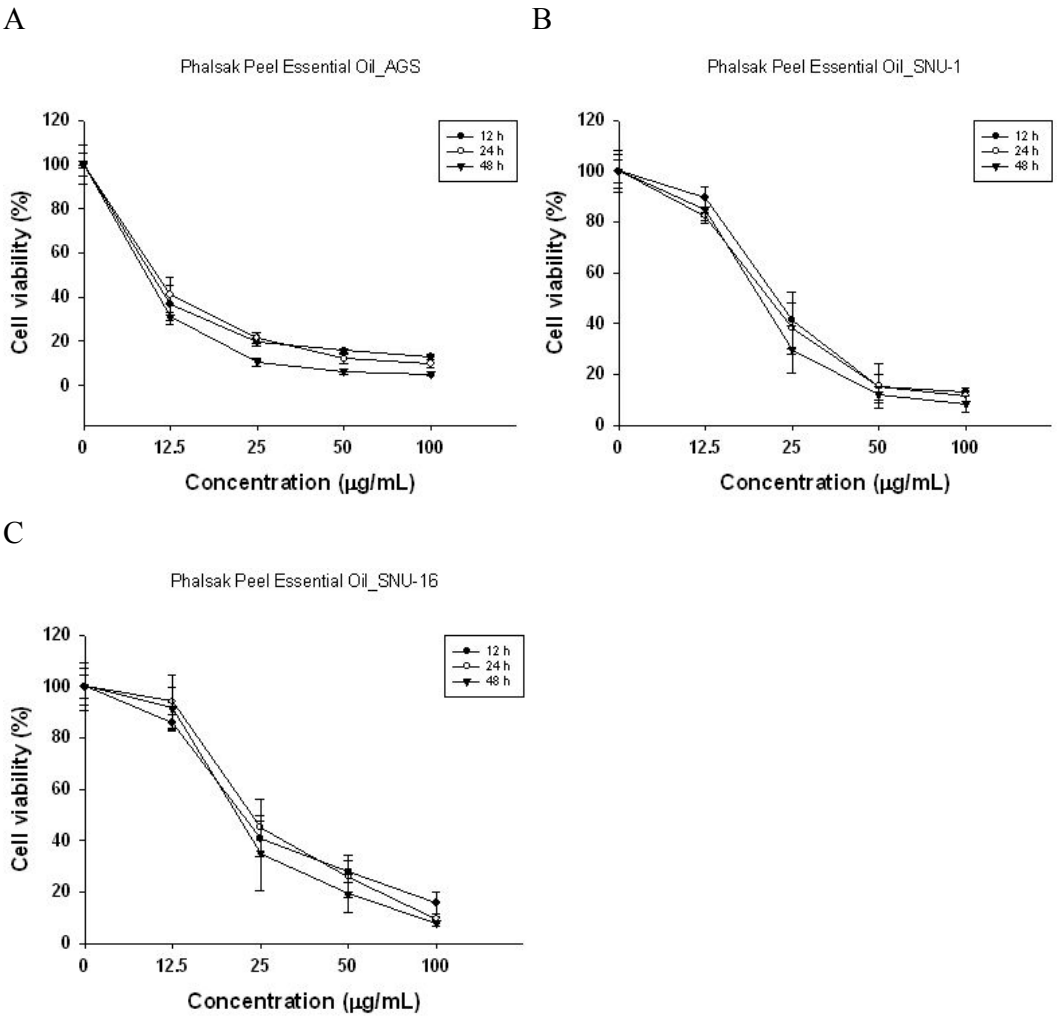

Figure. 2. Effect of the essential oil of phalsak (*Citrus hassaku* Hort ex Tanaka) peel on cell viability after 12, 24, and 48 h. (A) AGS, (B) SNU-1, (C) SNU-16. Untreated (DMSO alone) cells were used as controls.

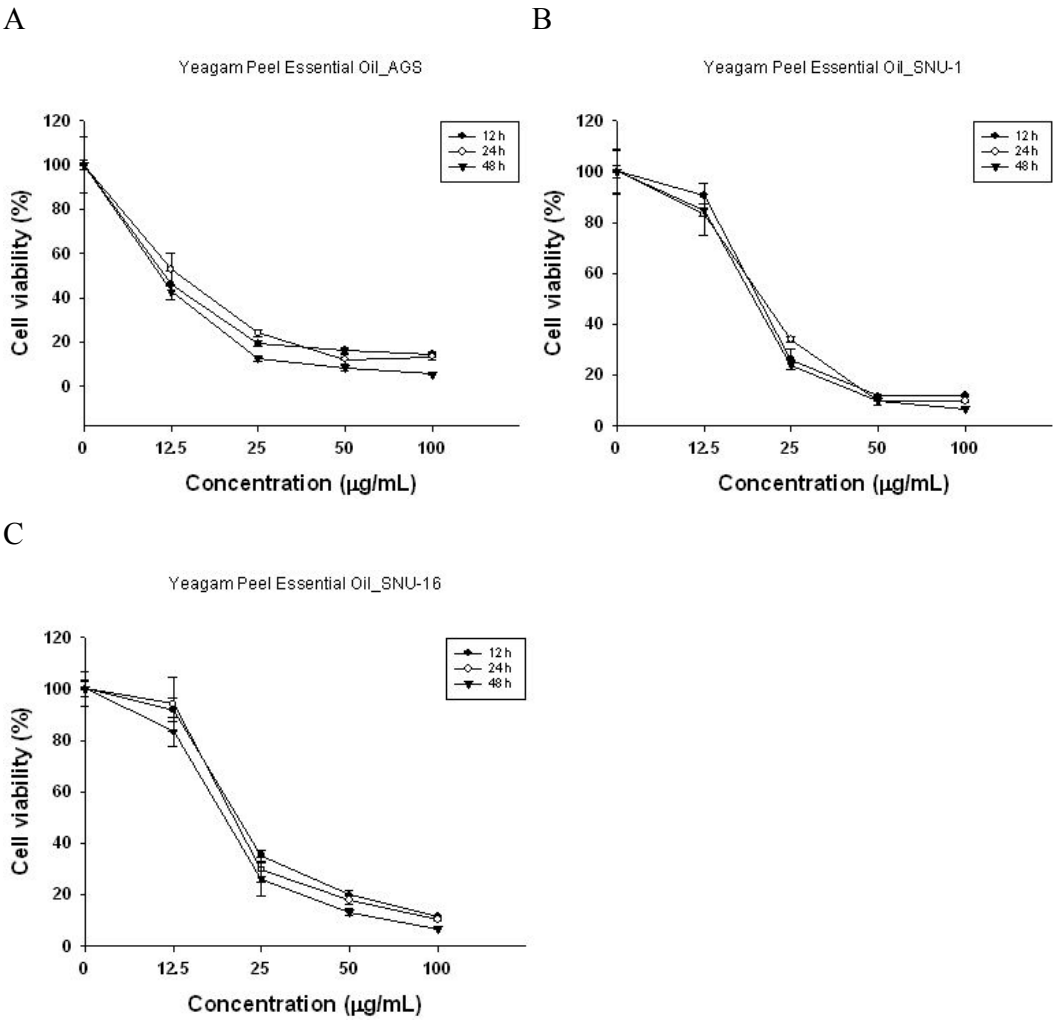

Figure. 3. Effect of the essential oil of yeagam (*Citrus iyo* Hort. ex Tanaka) peel on cell viability after 12, 24, and 48 h. (A) AGS, (B) SNU-1, (C) SNU-16. Untreated (DMSO alone) cells were used as controls.

4. 2. Chemical composition of Jeju *Citrus* essential oils

The analytical results of dangyuja, phalsak and yeagam peels essential oils are shown in Table 1 and Figure 4 (A-C), the principal components of the dangyuja *Citrus* peel oils were dl-limonene (64.69%), β-Myrcene (32.23%), and α-Pinene (0.49%); phalsak *Citrus* peel oils were dl-limonene (80.59%), γ-terpinene (5.04%), β-Myrcene (3.22%), p-cymene (2.28%), α-Pinene (1.80%), and β-pinene (1.28%); yeagam *Citrus* peel oils were dl-limonene (86.41%), γ-terpinene (6.64%), β-Myrcene (2.02%), linalool (1.69%), and α-Pinene (0.79%).

Table 1. Major components (in %) of Jeju *Citrus* peel oils separated by gas chromatography-mass spectroscopy.

RT	RI [a]	Name of the compound [b]	Area % [c]		
			dangyuja	phalsak	yeagam
10.486	928	α-Thujene	- [d]	0.39	0.15
10.765	932	α-Pinene	0.49	1.8	0.79
12.650	976	β-Phellandrene	-	-	0.07
12.659	976	Sabinene	0.07	0.18	-
12.773	978	β-Pinene	-	1.28	0.38
13.581	993	β-Myrcene	32.23	3.22	2.02
14.185	1004	n-Octanal	-	0.12	-
15.204	1027	p-Cymene	-	2.28	1.04
15.693	1036	dl-Limonene	64.69	80.59	86.41
16.440	1053	β-Ocimene	0.45	0.6	0.42
16.943	1063	γ-Terpinene	-	5.04	6.64
17.613	1076	Linalool oxide	0.4	0.11	-
18.398	1090	trans-Linalool oxide	0.2	-	-
18.403	1090	α-Terinolene	-	0.36	0.23
19.025	1101	Linalool	0.18	0.33	1.69
20.677	1127	Cis-Limonene oxide	-	0.25	-
20.907	1137	Z-limonene-1,2-epoxide	-	0.29	-
21.704	1157	Citronella	0.11	-	-
22.890	1180	4-Terpineol	-	0.12	-
23.574	1193	p-Menth-1-en-8-ol, (S)-(-)-	0.1	0.16	-
24.308	1207	n-Decanal	-	0.28	0.16
25.081	1224	BICYCLO[3.3.0]OCTAN-3-ON, 7-ETHYLIDEN-	0.1	-	-
26.042	1245	Z-Citral	0.04	-	-
26.178	1248	d-Carvone	-	0.19	-
27.474	1274	Citral	0.06	-	-
32.325	1379	α-Copaene	0.05	-	-

32.670	1386	Neryl acetate	0.09	-	-
34.286	1423	trans-Caryophyllene	0.1	-	-
36.974	1485	Germacrene-D	0.41	-	-
38.756	1528	δ-Cadinene	0.08	-	-
54.644	1956	Hexadecapentaene	0.11	-	-
55.798	1990	Farnesol	0.04	-	-

[a)] retention indices relative to C_7-C_{30} n-alkanes calculated on Rtx-5MS capillary column.

[b)] supercritical CO_2 extract of fruit compounds tentatively identified based on retention index and elution order as well as the fragmentation pattern described in the literature.

[c)] relative peak area percentage (peak area relative to the total peak area %)

-[d)], not detected

A

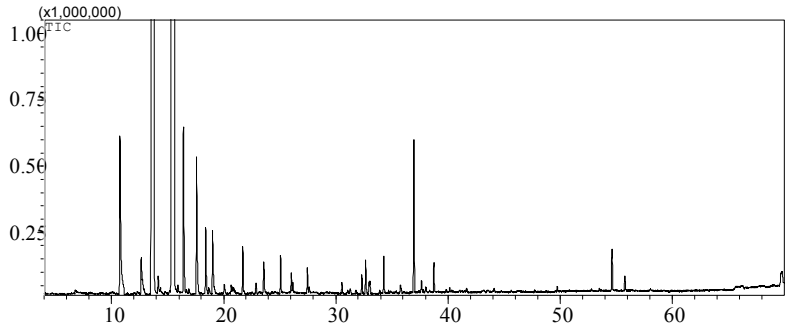

B

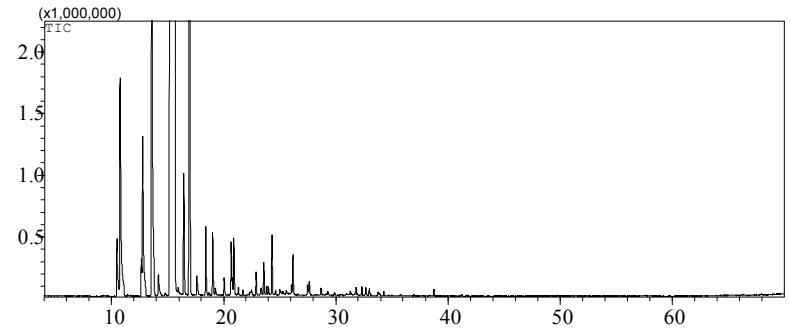

C

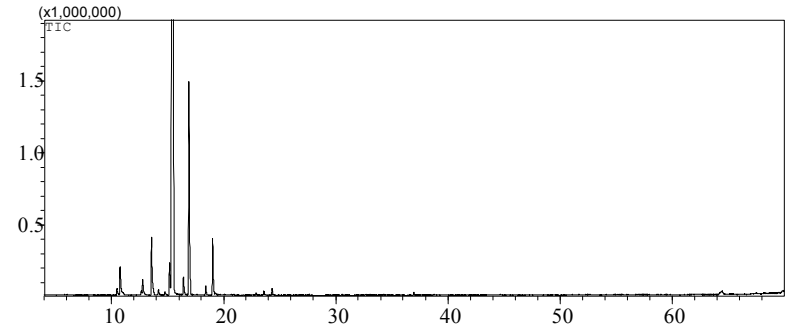

Figure. 4. GC-MS total ion chromatogram of Jeju *Citrus* peel Oils. (A) dangyuja (*Citrus* grandis Osbeck), (B) phalsak (*Citrus hassaku* Hort ex Tanaka), (C), yeagam (*Citrus* iyo Hort. ex Tanaka).

4. 3. Effect of major compounds of *Citrus* peel essential oils in human gastric cancer cells

We choose three compounds, major component of all EOs, dl-Limonene, α-Pinene, and β-Myrcene, and then performed MTT assay for measured proliferation of gastric cancer cells. As shown in Figure. 5, only dl-Limonen reduced the viability of all type of gastric cancer cells in a dose-dependent manner. IC_{50} values of dl-Limonene were 41.00, 113.60, and 113.06 in AGS, SNU-1 and SNU-16 for 24 h respectively. AGS was the most sensitive whereas, α-Pinene, and β-Myrcene dose not cytotoxic effect against SNU-1 and SNU-16, but slightly reduced cell viability on high concentration of these compounds in AGS (Fig. 5 A). Therefore, we suggest that dl-Limonen, major compound of Citrus peel EOs, is most important role of anti-proliferactive activity in gastric cancer cells.

A

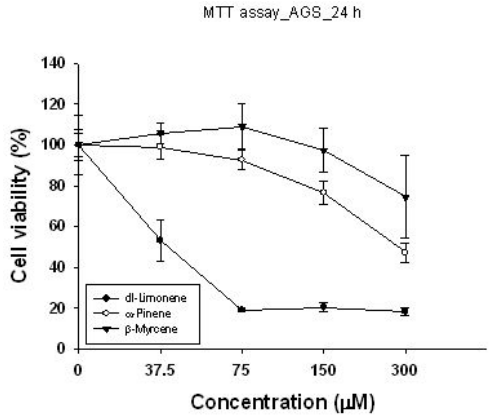

B

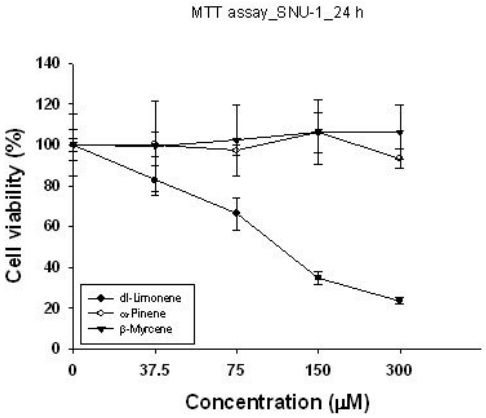

C

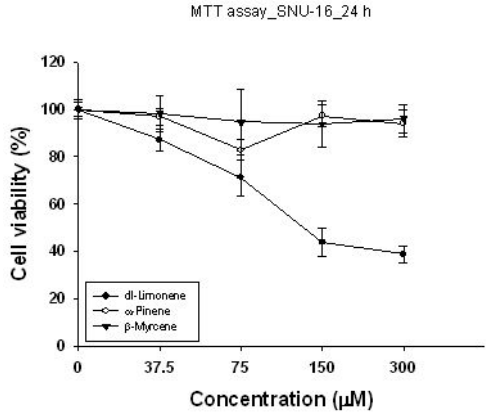

Figure. 5. Effect of Jeju *Citrus* EOs derived from compounds on cell viability after 24 h. (A) AGS, (B) SNU-1, (C) SNU-16. Untreated (DMSO alone) cells were used as controls.

5. DISCUSSION

Essential oils are generally extracted by distillation and steam distillation. Many kinds of essential oils are used in perfumes, cosmetics, soaps and other products, for flavoring food and drink, and for adding scents to incense and household cleaning products. In this study, we determined the compositional analysis and cytotoxic effect of essential oils from Jeju *Citrus* peels in a gastric cancer cell line. The results showed that all Jeju *Citrus* peel EOs appeared to have similar antiproliferaive effect on gastric cancer cell lines. Among them, most sensitive cell was, IC_{50} value were 14.83, 9.88, and 11.53 in danyuja, phalsak, and yeagam, respectively, AGS cells (Fig. 1A, 2A, and 3A).

In an investigation reported by (Lota *et al*., 2001) on *C.aurantium*, limonene was the most abundant compound of the peels EOs (87.6-95.1%) while other compounds were present at low amounts; α-Pinene (0.6%), β-pinene (2.4%) and myrcene (1.3-1.8%). In an investigation reported by (Leite *et al*., 2008) on *C. auranitum*, peels EOs contain limonene 96.24%, α-Pinene 0.53%, myrcene 2.24%, and linalool 0.44%. Our study revealed a slight difference in the compound of EOs among samples. The composition analysis results of dangyuja, phalsak and yeagam peels essential oils were as follows, the principal components of the dangyuja *Citrus* peel oils were dl-limonene (64.69%), β-Myrcene (32.23%), and α-Pinene (0.49%); phalsak *Citrus* peel oils were dl-limonene (80.59%), γ-terpinene (5.04%), β-Myrcene (3.22%), p-cymene (2.28%), α-Pinene (1.80%), and β-pinene (1.28%); yeagam *Citrus* peel oils were dl-limonene (86.41%), γ-terpinene (6.64%), β-Myrcene (2.02%), linalool (1.69%), and α-Pinene (0.79%).

dl-Limonene, a non-nutrient dietary component and major constituent in several *Citrus* oils and a number of other essential oils, has been found to inhibit the growth of cancer cells without toxicity. dl-Limonene, which comprises more than 90% of

orange peel oil, has chemopreventive and chemotherapeutic activities against rodent mammary, liver and pancreatic tumors (Elegbede *et al*., 1984; Kaji *et al*., 2001; Nakaizumi *et al*., 1997). As a result, cancer chemotherapeutic activities of pharmacological preparations of d-limonene are under evaluation of a phase I/II therapeutic clinical trial (McNamee *et al*., 1993). dl-Limonene, as a drug, is well tolerated in cancer patients at doses that may have clinical activity. A partial response in a breast cancer patient at a dose of 8 g/m^2/day was maintained for 11 months, and three additional patients with colorectal carcinoma showed stabilization of disease for longer than 6 months on dl-limonene at 0.5 or 1 g/m^2/day (Vigushin *et al*., 1998). The chemotherapeutic activity of d-limonene may be due to induction of apoptosis and redifferentiation concomitant with increased expression of mannose-6-phosphate/insulin-like growth factor II receptor and transforming growth factor B1 (Jirtle RL *et al*., 1993). dl-Limonene and its *in vivo* plasma metabolites have been shown to be the inhibitors of protein isoprenylation of small G proteins, including p21 ras in rats (Bourne *et al*., 1991). In addition to selectively blocking the isoprenylation of small G proteins, dl-limonene has also been shown to have additional cellular effects, including the inhibition of coenzyme Q synthesis, and it is also capable of causing the complete regression of the majority of advanced primary rat mammary carcinomas without significant toxicity (Haag *et al*., 1992). We performed MTT assay result was dl-Limonen reduced the viability of all type of gastric cancer cells in a dose-dependent manner. In the AGS cells, α-Pinene, and β-Myrcene were slightly reduced cell viabiltiy, in the contrast, did not cytotoxic effect against SNU-1 and SNU-16.

PART III

Super Critical Extracts of Jeju traditional *Citrus*

1. **Antiproliferative activities of Super Critical Extracts (SCE) in AGS cells**
2. **Compositional analysis of Super Critical Extract**
3. **Antiproliferative activity of Auraptene and its Mechanism in SNU-1 Human Gastric Cancer Cell**

1. ABSTRACT

Supercritical CO_2 extract from fruits of *Citrus grandis* Osbeck, *Citrus hassaku* Hort ex Tanaka, and *Citrus iyo* Hort. ex Tanaka locally known as dangyuja, phalsak, and yeagam, respectively, in Korea, were analyzed by gas chromatography-mass spectrometry (GC–MS). In total, (48, 54), (50, 58), and (26, 34) compounds were identified in flesh and peel of dangyuja, phalsak, and yeagam, respectively. Antiproliferative activity of the flesh and peel extracts were revealed through the colorimetric MTT (tetrazolium) assay against gastric cancer cell lines. Although all tested peel extracts exhibited antiproliferative effects toward cancer cells, different cell lines varied in their sensitivity to the same plant fruit extract. In addition, auraptene identified from phalsak peel SCE significant induced apoptosis in SNU-1 cells. However, auraptene was induced caspase-dependent apoptosis whereas increase phosphorylation of Akt by westernblot analysis. Also, mTOR kinase inhibition causes feedback-dependent phosphorylation of Akt by mTOR inhibitor, rapamycin. Based on the results, we suggest that while caspase-dependent apoptosis was induced, auraptene-induced mTOR activity process also diminished in SNU-1 cells. In conclusion, *Citrus* peel SCEs were more inhibit the antiproliferative effects than flesh SCEs, and auraptene, one of the compound in *Citrus* SCEs, cause apoptosis in SNU-1 cells and suggests that auraptene acts as a mTOR inhibitor reaction.

2. INTRODUCTION

The supercritical extraction method is a more promising process to obtain volatile and non-volatile compounds by avoiding thermal degradation and solvent residue in the extracts (Ranalli *et al*., 2004). Compared to conventional methods, this method is the most useful in terms of essential oil and polymethoxylated flavonoid yields from *Citrus* fruits (Porta *et al*., 1997; Li *et al*., 2007; Atti-Santos *et al*., 2005). The presence of polymethoxy flavone, unsaturated fatty acids, and phytosterols along with several terpenoids in *Citrus* extracts are particularly important because they promote the anticancer effects. Although many benefits of supercritical extracts have been claimed, there is a dearth of information about the chemical profiles and antiproliferative activity of Korean *Citrus* fruits extracted using this method.

Supercritical fluid extraction, supercritical gas extraction, and dense gas extraction are alternative terms to name the operation with a fluid at temperatures and pressures near the critical point. In comparison with conventional, liquid organic solvents, supercritical fluids have a higher diffusivity and lower density, viscosity, and surface tension. On the other hand, the properties of supercritical fluids can be varied over a wide range by changing the operational conditions. CO_2 [(Pc) 7.28 MPa; (Tc) 304.1 K] is the most frequently used solvent for SCE, because of its practical advantages (including its nontoxic and nonflammable character, environmental safety, huge availability, low cost at high purity, and suitability for extracting heat labile, natural compounds with low volatility and polarity). When the extract is recovered in the separators, CO_2 is easily separated because of its high volatility. For conventional extraction methods such as hydrodistillation (steam distillation) and solvent extraction, there are few adjustable parameters to control the selectivity of the extraction processes. Therefore, developing alternative extraction techniques with better selectivity and efficiency are highly desirable. Consequently, supercritical extraction (SCE) as an environmentally responsible and efficient extraction technique

for solid materials was introduced and extensively studied for separation of active compounds from herbs and other plants (Modey *et al*., 1996). The high solvation power of supercritical extracts (SCEs) was first reported over a century ago (Hannay and Hogarth, 1879). In recent years, SCE has received a great deal of attention as the full potential of this technology in analytical applications has begun to emerge (Smith, 1988; Rein and Cork, 1991). Today, SCE has become an acceptable extraction technique used in many areas. SCE of active natural products from herbal or more generally, from plant materials has become one of the most important application areas (McHugh and Krukonis, 1994; Luque de Castro *et al*., 1994). With the increasing public interest in herbal medicines and natural products, numerous SCE-related research papers in herbal or natural product studies have been published in recent years. In this study, we investigated that SCEs induced decrease of gastric cancer cells growth and how auraptene, major compound of phalsak peel SCE, affects induced gastric cancer cell death mechanism.

3. MATERIALS AND METHODS

3. 1. Plant materials

Fruits of *Citrus grandis* Osbeck, *Citrus hassaku* Hort ex Tanaka, and *Citrus* iyo Hort. ex Tanaka locally known as dangyuja, phalsak, and yeagam respectively were collected from the National Institute of Subtropical Agriculture, Jeju Province, Korea. Botanical samples were previously taxonomically identified, and voucher specimens were deposited in the laboratory of Dr. S.K. Cho at the College of Applied Life Sciences, Jeju National University.

3. 2. Supercritical fluid extraction

Peel and flesh of dangyuja, phalsak, and yeagam were loaded separately into a 1 L thick-walled stainless steel thimble extraction cell and extracted at 50^{o}C for 2 h. The extraction was performed using CO_2 at 300 bar pressure in a diaphragm compressor (Haskel Co. Bellingham, WA, USA). The extracts were deposited in a separator attached to a metering valve and held in a circulating bath at 0^{o}C. Finally, the extracts were collected into a clean vial and stored at -20^{o}C until analysis.

3. 3. GC-MS analysis

Chromatographic analysis was carried out using a Shimadzu GC-MS (model QP-2010, Shimadzu Co., Kyoto, Japan) attached to AOC-5000 autosampler in electron impact mode. The ionization voltage was 70 eV, and the temperatures of the injector and interface were 250^{o}C and 290^{o}C respectively. The capillary column used was an Rtx-5MS (30 m length, 0.25 mm internal diameter, and 0.25 μm film thickness). The oven temperature was programmed at 60^{o}C (isothermal for 2 min) and was ramped to 250^{o}C at 5^{o}C/min and to 310^{o}C at 8^{o}C/min (isothermal for 12 min). Helium was used as the carrier gas at a flow rate of 1 mL/min with 57.4 kPa pressure, and an injector volume of 1 μL using a 1:10 split ratio. Mass range was from m/z 40-500 amu. The

extracts of the fruits were solubilized in n-hexane, filtered through a 0.20-μm syringe filter (Advantec, Tokyo, Japan), and aliquots were injected into the GC-MS. Mass spectra of each compound were tentatively identified with the mass spectral data contained within the WILEY7 and NIST05 libraries and by their Kovats indices relative to C_7-C_{30} n-alkanes (Sigma-Aldrich Chemie GmbH, Steinheim, Germany) on an Rtx-5MS column. Further tentative identification was completed by comparing the mass spectra with those of authentic standards (Adams, 1989).

3. 4. Cell culture

Gastric cancer (AGS, MKN45, SNU-1, and SNU-16) cells were maintained at 37ºC in a humidified atmosphere under 5% CO_2 in F12K or RPMI 1640 containing 10% heat-inactivated FBS, 100 U/mL penicillin, and 100 μg/mL streptomycin. Exponentially grown cells were treated with various concentrations of the solvent fractions, as indicated.

3. 5. Cell viability assay

Cells were maintained in a humidified incubator at 37°C in a 5% CO_2 atmosphere. Antiproliferative activity was determined by the cell viability assay. The effect of the samples on the viability of various cancer cell lines was determined by a MTT-based assay. Exponential-phase cells were collected and transferred to a microtiter plate (2×10^3- 5×10^4 cells per mL) to detect cytotoxicity in the gastric cancer cell lines. The cells were incubated for 2 days with various concentrations of the fruit extract. The supercritical extract was dissolved in DMSO and diluted in PBS to obtain a stock solution, which was stored at -20°C. After the incubation, 0.1 mg MTT (Sigma, St. Louis, MO, USA) was added to each well, and the cells were incubated at 37°C for 4 h. The medium was carefully removed. DMSO (150 μL) was added to each well to dissolve the formazan crystals. The plates were read at 570 nm after the crystal had dissolved completely, using a Sunrise microplate reader (Sunrise, Tecan, Salzburg,

Austria). The percent cell viability was calculated based on the following formula: mean value of (control group - treated group/control group) × 100%. All results were assessed in triplicate for each concentration.

3. 6. Microscopic observation of cellular morphology

Gastric cancer cells, placed in 6-well plates at 5×10^4 cells/mL, were treated with the samples. After 24 h, 10 μM of Hoechst 33342 a DNA-specific fluorescent dye, were added to the solution in each well and the plates were incubated for 10 min at 37°C. The stained cells were then observed under an Olympus fluorescence microscope.

3. 8. Flow cytometric analysis

To determine cell cycle distribution analysis, 5×10^4 cells/mL were plated in 6 well plate, treated with the samples for 24 h. After treatment, the cells were collected, fixed in 70% ethanol, washed in PBS (2 mM EDTA), resuspended in 1 mL PBS containing 1 mg/mL RNase and 50 mg/mL propidium iodide, incubated in the dark for 30 min at 37°C, and analyzed by FACS caliber flow cytometry (Becton Dickinson, USA). Data from 10,000 cells were collected for each data file.

3. 9. Westernblot analysis

After treatment, the cells were collected and washed twice with cold PBS. The cells were then lysed in lysis buffer (50 mM Tris-HCl, pH 7.5, 150 mM NaCl, 1% Nonidet P-40, 2 mM EDTA, 1 mM EGTA, 1 mM $NaVO_3$, 10 mM NaF, 1 mM DTT, 1 mM PMSF, 25 μg/mL aprotinin, and 25 μg/mL leupeptin) and kept on ice for 30 min. The lysates were then centrifuged at 13,000 × rpm at 4°C for 30 min; the supernatants were stored at -70°C until use. The protein concentration was determined by the bicinchoninic acid (BCA) protein assay kit (Pierce, Rockford, IL,

USA). Aliquots of the lysates (60-100 μg of protein) were separated by 7.5-15% SDS-PAGE and transferred onto a polyvinylidine difluoride (PVDF) membrane (Bio-RAD, HC, USA) using a glycine transfer buffer (192 mM glycine, 25 mM Tris-HCl, pH 8.8, and 20% methanol [v/v]). After blocking with 5% nonfat dried milk, the membrane was incubated for 2 h with primary antibodies followed by 30 min with secondary antibodies in milk containing Tris-buffered saline (TBS) and 0.1% Tween 20. All primary antibodies were used at a dilution of 1:1,000; HRP-conjugated goat anti-rabbit IgG (H+L) and HRP-conjugated goat anti-mouse IgG were used as secondary antibodies at a dilution of 1:5,000. The PVDF membrane was then exposed to X-ray film (AGFA, Mortsel, Belgium), and the protein bands were detected using a WEST-ZOL® plus Western Blot Detection System (iNtRON, Gyeonggi-do, Korea).

4. RESULTS

4.1 Cytotoxic effect of SCEs

Antiproliferative activity was evaluated by monitoring cell viability of treated cancer cells by cell count or reduction of the tetrazolium substrate to formazan. MTT assay was carried out to investigate the cytotoxic effect of SCEs of Citrus, Citrus grandis Osbeck (dangyuja), Citrus hassaku Hort ex Tanaka (phalsak), and Citrus iyo Hort (yeagam), peel and flesh against human gastric cancer cells. Gastric cancer cell AGS was taken as representative cells for the screening purpose. Cytotoxic effect of immature fruit was slightly greater than that of mature fruit and the effect of the peel fraction was significantly greater than the flesh fraction against the gastric cancer cells (Fig. 6). We noticed that immature Citrus hassaku Hort ex Tanaka (phalsak) peel of SCEs components seems to be more efficient than that of the flesh against AGS cells. Therefore, we performed that find the main compounds in the immaturee Citrus peel SCE by using the GC/MS.

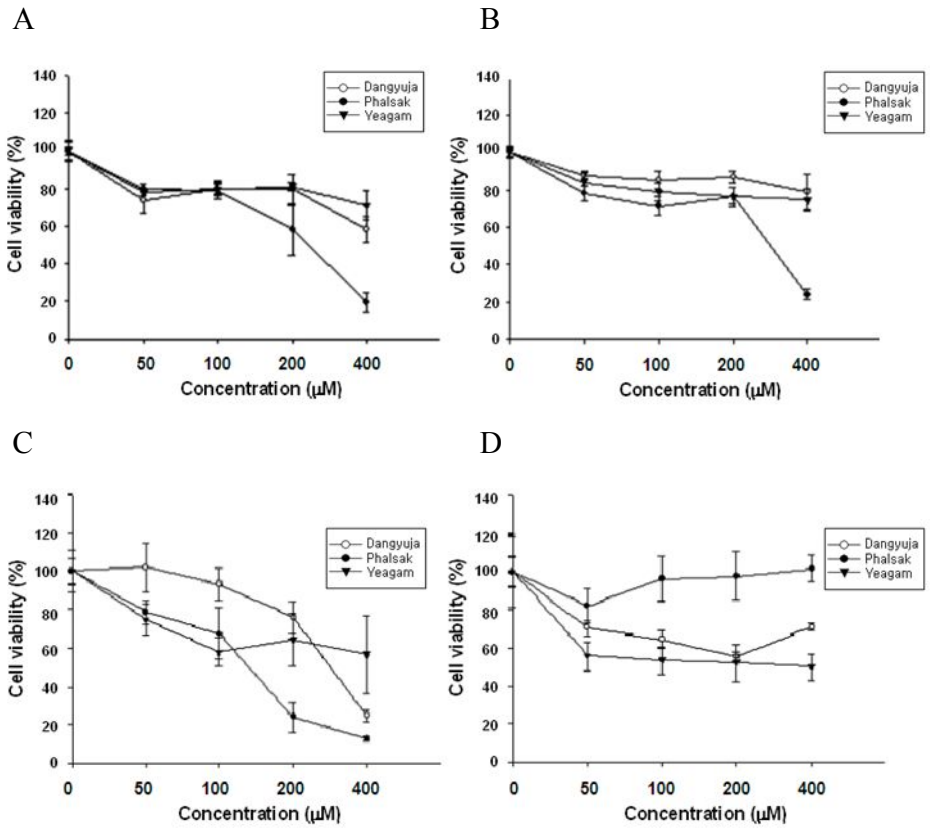

Figure. 6. Effect of the SCEs of Jeju *Citrus grandis* Osbeck (dangyuja), *Citrus hassaku* Hort ex Tanaka (phalsak), and *Citrus iyo* Hort. ex Tanaka (yeagam) peel and flesh on cell viability after 48 h in AGS cells. SCEs of Mature *Citrus* peel and flesh, respectively (A and B). SCEs of Immature *Citrus* peel and flesh, respectively (C and D).

4.2. Chemical constituents of Jeju *Citrus* Supercritical Extracts

The GC/MS analysis of peel SCEs revealed 58, 54, 64 and 34, 31, 29 compounds in mature and immature of dangyuja (Table 2, 3 and Fig. 7), phalsak (Table 4, 5 and Fig. 8) and yeagam (Table 6, 7 and Fig. 9), respectively. And flesh SCEs revealed 50, 48, 53 and 26, 27, 27 compounds in mature and immature of dangyuja (Table 2, 3 and Fig. 7), phalsak (Table 4, 5 and Fig. 8) and yeagam (Table 6, 7 and Fig. 9), respectively. We analysis mature and immature SCEs and major compounds were limonene, beta-myrcene, linanool, γ-Sitosterol, (Z,Z)-9,12-Octadecanoic acid ethyl ester, Germacrene-D , Hexadecanoic acid , Caryophyllene oxide and so on. In immature state, there are lots of difference composition between peel and flesh. Moreover, phalsak peel SCE showed dramatic inhibition of cell growth in AGS, compared to other peel SCEs. Among the components of phalsak SCEs, auraptene was found in both peel and flesh SCEs but the proportions was a great difference between peel and flesh (Table 4, 5, and Fig. 8).

Table 2. Chemical compounds identified from supercritical extract of mature dangyuja variety

SN	RT	RI [a]	Name of the compound [b]	MF	Area% [c]	
					Peel	Flesh
1.	7.78	991	β-pinene	$C_{10}H_{16}$	0.50	1.01
2.	7.85	993	β-Myrcene	$C_{10}H_{16}$	0.05	0.91
3.	7.90	995	(E,E)-2,4-Heptadienal	$C_7H_{10}O$	- [d]	0.56
4.	8.97	1034	Limonene	$C_{10}H_{16}$	3.63	3.93
5.	10.99	1100	Linalool	$C_{10}H_{18}O$	0.78	0.18
6.	11.08	1103	Nonanal	$C_9H_{18}O$	-	0.16
7.	12.07	1138	(*Z*)-Limonene oxide	$C_{10}H_{16}O$	0.05	0.04
8.	12.19	1142	(*E*)-limonene oxide	$C_{10}H_{16}O$	0.07	0.06
9.	12.60	1156	Citronellal	$C_{10}H_{18}O$	0.33	-
10.	13.81	1193	α-Terpineol	$C_{10}H_{18}O$	0.88	0.15
11.	14.64	1222	Carveol	$C_{10}H_{16}O$	0.09	0.15
12.	14.84	1229	β-Citronellol	$C_{10}H_{20}O$	0.44	-
13.	15.25	1244	β-Citral	$C_{10}H_{16}O$	0.22	0.09
14.	15.61	1256	α-Geraniol	$C_{10}H_{18}O$	0.59	0.06
15.	15.78	1262	(E)-2-Decenal	$C_{10}H_{18}O$	-	0.61
16.	16.11	1273	α-Citral	$C_{10}H_{16}O$	0.68	0.09
17.	16.78	1295	(E,Z)-2,4-Decadienal	$C_{10}H_{16}O$	0.89	4.50
18.	17.44	1319	(E,E)-2,4-Decadienal	$C_{10}H_{16}O$	1.28	6.32
19.	18.38	1353	Citronellyl acetate	$C_{12}H_{22}O_2$	0.51	-
20.	18.66	1363	2-Undecenal	$C_{11}H_{20}O$	-	0.60
21.	18.69	1364	Neryl acetate	$C_{12}H_{20}O_2$	0.39	-
22.	19.24	1383	Geranyl acetate	$C_{12}H_{20}O_2$	4.36	0.3
23.	19.55	1394	Tetradecane	$C_{14}H_{30}$	-	0.16
24.	19.56	1395	β-Cubebene	$C_{15}H_{24}$	0.83	-
25.	20.02	1412	Dimethyl anthranilate	$C_9H_{11}NO_2$	-	0.14
26.	20.05	1413	Perillyl acetate	$C_{12}H_{18}O_2$	0.23	-
27.	20.42	1428	β-Caryophyllene	$C_{15}H_{24}$	0.39	0.10
28.	21.09	1453	(E)-Geranylacetone	$C_{13}H_{22}O$	0.38	0.76

29.	21.32	1462	α-Humulene	$C_{15}H_{24}$	0.10	-
30.	22.04	1488	Germacrene D	$C_{15}H_{24}$	0.06	-
31.	22.17	1495	Pentadecane	$C_{15}H_{32}$	-	0.23
32.	22.66	1513	2,4-Di-tert-butylphenol	$C_{14}H_{22}O$	0.40	0.43
33.	23.07	1530	δ-Cadinene	$C_{15}H_{24}$	1.06	0.10
34.	23.37	1542	Dihydroactinidiolide	$C_{11}H_{16}O_2$	0.33	-
35.	23.80	1559	Dodecanoic acid	$C_{12}H_{24}O_2$	0.5	0.19
36.	24.53	1588	Spathulenol	$C_{15}H_{24}O$	0.97	0.04
37.	24.66	1595	Hexadecane	$C_{16}H_{34}$	-	0.16
38.	24.69	1594	Caryophyllene oxide	$C_{15}H_{24}O$	1.41	0.22
39.	24.89	1604	Salvial-4(14)-en-1-one	$C_{14}H_{22}O$	0.13	-
40.	28.53	1760	Tetradecanoic acid	$C_{14}H_{28}O_2$	0.58	0.25
41.	29.90	1822	Nootkatone	$C_{15}H_{22}O$	1.50	-
42.	31.02	1874	Platambin	$C_{15}H_{26}O_2$	0.64	-
43.	31.92	1917	(E,E)-Farnesyl acetone	$C_{18}H_{30}O$	0.55	-
44.	32.04	1923	Pentadecanoic acid, methyl ester	$C_{16}H_{32}O_2$	1.57	4.74
45.	32.98	1969	Hexadecanoic acid	$C_{16}H_{32}O_2$	3.72	9.94
46.	33.37	1990	Hexadecanoic acid, ethyl ester	$C_{17}H_{34}O_2$	2.96	0.94
47.	35.17	2076	Xanthotoxin	$C_{12}H_8O_4$	0.74	-
48.	35.42	2095	(Z,Z)-9,12-Octadecadienoic acid, methyl ester	$C_{19}H_{34}O_2$	1.44	2.39
49.	35.53	2101	(Z)-9-Octadecenoic acid methyl ester	$C_{19}H_{36}O_2$	0.09	0.81
50.	36.41	2149	(Z,Z)-9,12-Octadecadienoic acid, ethyl ester	$C_{20}H_{36}O_2$	4.54	4.28
51.	36.72	2163	(Z)-9-Octadecenoic acid ethyl ester	$C_{20}H_{38}O_2$	0.37	1.46
52.	37.28	2195	Docosane	$C_{22}H_{46}$	0.38	1.41
53.	39.10	2296	Tricosane	$C_{23}H_{48}$	0.54	6.16
54.	40.75	2396	Tetracosane	$C_{24}H_{50}$	0.35	3.65
55.	42.27	2494	Pentacosane	$C_{25}H_{52}$	0.67	7.02
56.	43.60	2593	Hexacosane	$C_{26}H_{54}$	0.38	4.17
57.	44.33	2655	Auraptene	$C_{19}H_{22}O_3$	1.71	-
58.	45.60	2798	Octacosane	$C_{28}H_{58}$	0.12	1.24
59.	46.35	2833	Squalene	$C_{30}H_{50}$	1.94	0.65

60.	48.93	3000<	Hentriacontane	$C_{31}H_{64}$	0.23	0.15
61.	49.79	3000<	Vitamin E	$C_{29}H_{50}O_2$	0.21	0.08
62.	50.73	3000<	Tangeritin	$C_{20}H_{20}O_7$	1.24	0.56
63.	51.38	3000<	δ5-Ergostenol	$C_{28}H_{48}O$	1.30	1.19
64.	51.81	3000<	Stigmasterol	$C_{29}H_{48}O$	1.01	0.54
65.	52.75	3000<	γ-Sitosterol	$C_{29}H_{50}O$	5.09	3.59
66.	53.43	3000<	Nobiletin	$C_{21}H_{22}O_8$	0.53	-

[a)] retention indices relative to C_7-C_{30} n-alkanes calculated on Rtx-5MS capillary column.

[b)] supercritical CO_2 extract of fruit compounds tentatively identified based on retention index and elution order as well as the fragmentation pattern described in the literature.

[c)] relative peak area percentage (peak area relative to the total peak area %)

-[d)], not detected

Table 3. Chemical compounds identified from supercritical extract of immature dangyuja variety

SN	RT	RI [a]	Name of the compound [b]	MF	Area% [c]	
					Peel	Flesh
1.	7.81	992	β-Myrcene	$C_{10}H_{16}$	12.41	- [d]
2.	8.98	1035	Limonene	$C_{10}H_{16}$	13.09	1.73
3.	11.01	1100	Linalool	$C_{10}H_{18}O$	1.94	-
4.	13.78	1193	α-Terpineol	$C_{10}H_{18}O$	0.65	-
5.	15.21	1243	Z-Citral	$C_{10}H_{16}O$	0.25	-
6.	15.56	1255	trans-Geraniol	$C_{10}H_{18}O$	0.23	-
7.	18.06	1342	δ-Elemene	$C_{15}H_{24}$	0.78	-
8.	19.19	1382	Geranyl acetate	$C_{12}H_{20}O_2$	1.55	-
9.	19.53	1394	β-Elemene	$C_{15}H_{24}$	0.98	-
10.	20.41	1427	β-Caryophyllene	$C_{15}H_{24}$	1.55	-
11.	21.14	1456	Nerolidol	$C_{15}H_{26}O$	0.39	-
12.	21.27	1461	α-Humulene	$C_{15}H_{24}$	0.43	-
13.	22.04	1489	Germacrene-D	$C_{15}H_{24}$	3.79	-
14.	22.40	1502	Bicyclogermacrene	$C_{15}H_{24}$	0.34	-
15.	22.60	1511	2,4-Di-tert-butylphenol	$C_{15}H_{22}O$	0.26	0.4
16.	23.06	1530	δ-Cadinene	$C_{15}H_{24}$	0.77	-
17.	23.66	1554	Elemol	$C_{15}H_{26}O$	0.45	-
18.	27.16	1699	β-Sinensal	$C_{15}H_{22}O$	0.24	-
19.	28.43	1756	α-Sinensal	$C_{15}H_{22}O$	0.42	-
20.	32.78	1960	Hexadecanoic acid	$C_{16}H_{32}O2$	-	4.32
21.	35.14	2079	Xanthotoxin	$C_{12}H_8O_4$	1.18	0.3
22.	35.35	2090	Henicosane	$C_{21}H_{44}$	-	0.47
23.	35.77	2112	Phytol	$C_{20}H_{40}O$	0.23	-
24.	36.23	2137	Ethyl linoleate	$C_{20}H_{36}O_2$	-	4.75
25.	36.36	2144	Octadecanoic acid	$C_{18}H_{36}O_2$	-	3.69
26.	36.56	2155	Osthol	$C_{15}H_{16}O_3$	0.95	-
27.	37.22	2189	Docosane	$C_{22}H_{46}$	-	0.98
28.	38.45	2259	7-Methoxy-8-(2-oxo-3-	$C_{15}H_{16}O_4$	1.28	-

			methylbutyl)coumarin			
29.	38.67	2271	1,1,4,4-Tetramethyl-2-tetralone	$C_{14}H_{18}O$	17.84	-
30.	39.06	2293	Tricosane	$C_{23}H_{48}$	-	7.07
31.	39.25	2304	7-Methoxy-8-(2-oxo-3-methylbutyl)coumarin	$C_{15}H_{16}O_4$	0.87	-
32.	40.08	2354	2-Methyltricosane	$C_{24}H_{52}$	-	1.14
33.	40.27	2365	9-Butyldocosane	$C_{26}H_{54}$	-	3.77
34.	40.70	2390	Tetracosane	$C_{24}H_{50}$	-	3.05
35.	41.68	2455	Methyl-tetracosane	$C_{25}H_{50}$	-	5.99
36.	42.25	2493	Pentacosane	$C_{25}H_{52}$	-	8.24
37.	43.58	2593	Hexacosane	$C_{26}H_{54}$	-	1.30
38.	44.29	2652	Auraptene	$C_{19}H_{22}O_3$	3.66	0.96
39.	44.32	2654	8-Methylhexacosane	$C_{27}H_{54}$	-	2.07
40.	44.8	2693	Heptacosane	$C_{27}H_{56}$	-	2.03
41.	46.35	2829	Squalene	$C_{30}H_{50}$	-	0.78
42.	47.88	3000	Triacontane	$C_{30}H_{62}$	-	0.21
43.	48.78	3000<	γ-Tocopherol	$C_{28}H_{48}O_2$	1.00	-
44.	49.78	3000<	α-Tocopherol	$C_{28}H_{48}O_2$	4.41	-
45.	50.71	3000<	4',5,6,7,8-Pentamethoxyflavone	$C_{20}H_{20}O_7$	2.8	0.66
46.	51.38	3000<	δ-5-Ergostenol	$C_{28}H_{48}O$	2.03	3.02
47.	52.73	3000<	γ-Sitosterol	$C_{29}H_{48}O$	1.96	1.22
48.	52.69	3000<	γ-Sitosterol	$C_{29}H_{50}O$	8.11	11.38
49.	53.09	3000<	3,3',4',5,5',7,8-Heptamethoxyflavone	$C_{22}H_{24}O_9$	2.4	0.87
50.	53.43	3000<	3',4',5,6,7,8-Hexamethoxyflavone	$C_{21}H_{22}O_8$	1.48	0.66

[a)] retention indices relative to C_7-C_{30} n-alkanes calculated on Rtx-5MS capillary column.

[b)] supercritical CO_2 extract of fruit compounds tentatively identified based on retention index and elution order as well as the fragmentation pattern described in the literature.

[c)] relative peak area percentage (peak area relative to the total peak area %)

-[d)], not detected

A

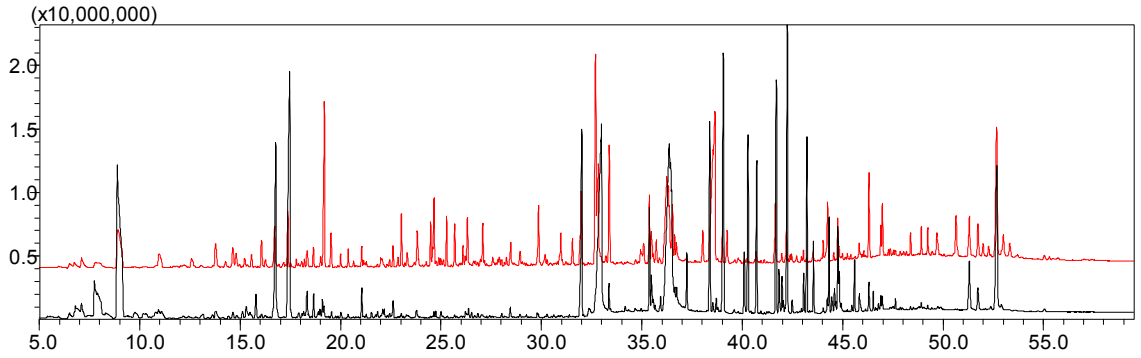

B

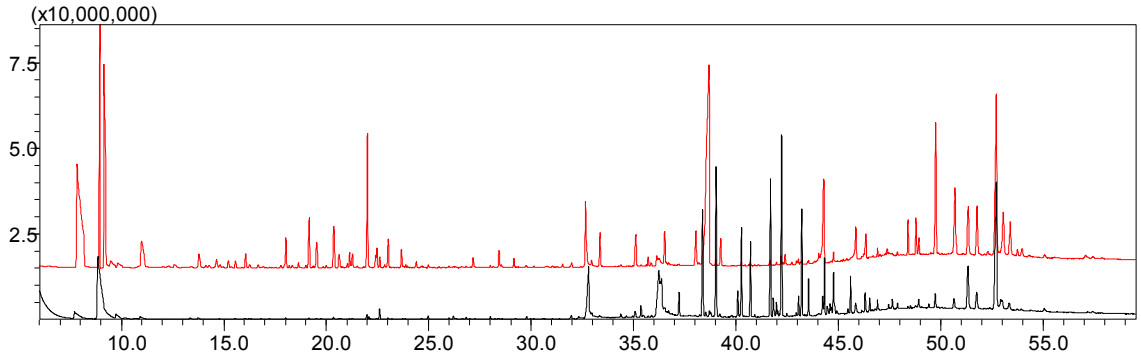

Figure. 7. GC-MS chromatogram of supercritical extract of dangyuja varieties from Jeju, Korea. A: Mature *Citrus* SCEs, B: Immature *Citrus* SCEs. (Red : peel, Black : flesh)

Table 4. Chemical compounds identified from supercritical extract of mature phalsak variety

SN	RT	RI [a]	Name of the compound [b]	MF	Area% [c]	
					Peel	Flesh
1.	7.83	993	β-Myrcene	$C_{10}H_{16}$	0.22	- [d]
2.	8.77	1027	p-Cymene	$C_{10}H_{14}$	0.03	0.03
3.	8.90	1032	Limonene	$C_{10}H_{16}$	0.25	0.35
4.	9.78	1062	2-Octenal	$C_8H_{14}O$	0.05	0.49
5.	10.65	1090	Linalool oxide	$C_{10}H_{18}O_2$	0.15	0.09
6.	10.97	1099	Linalool	$C_{10}H_{18}O$	0.38	0.85
7.	13.18	1174	Octanoic acid	$C_8H_{16}O_2$	0.15	0.28
8.	13.41	1181	4-Terpineol	$C_{10}H_{18}O$	0.08	0.06
9.	13.80	1193	α-Terpineol	$C_{10}H_{18}O$	1.38	0.41
10.	15.775	1262	(E)-2-Decenal	$C_{10}H_{18}O$	-	0.21
11.	16.09	1272	α-Citral	$C_{10}H_{16}O$	0.33	0.06
12.	16.29	1279	Perilla aldehyde	$C_{10}H_{14}O$	0.34	0.05
13.	16.76	1294	(*E,Z*)2,4-Decadienal	$C_{10}H_{16}O$	1.93	0.98
14.	17.42	1318	(*E,E*)-2,4-Decadienal	$C_{10}H_{16}O$	2.79	1.81
15.	18.36	1352	Citronellyl acetate	$C_{12}H_{22}O_2$	0.36	-
16.	18.65	1362	2-Undecenal	$C_{11}H_{20}O$	-	0.28
17.	18.68	1364	Neryl acetate	$C_{12}H_{20}O_2$	0.97	-
18.	19.20	1381	Geranyl acetate	$C_{12}H_{20}O_2$	1.33	0.22
19.	19.56	1391	β-Cubebene	$C_{15}H_{24}$	0.58	-
20.	19.89	1406	Decyl acetate	$C_{12}H_{24}O_2$	0.58	0.05
21.	20.03	1412	Prillyl acetate	$C_{12}H_{18}O_2$	0.37	0.06
22.	20.37	1426	(E)-Caryophyllene	$C_{15}H_{24}$	0.19	-
23.	21.08	1453	(E)-Geranylacetone	$C_{13}H_{22}O$	0.34	0.16
24.	21.14	1456	Citronellol	$C_{10}H_{20}O$	0.95	-
25.	22.16	1493	Pentadecane	$C_{15}H_{32}$	-	0.06
26.	22.66	1512	2,4-Di-tert-butylphenol	$C_{14}H_{22}O$	0.56	0.4
27.	23.06	1529	δ-Cadinene	$C_{15}H_{24}$	1.51	0.03
28.	23.36	1541	Dihydroactinidiolide	$C_{11}H_{16}O_2$	0.31	0.15

29.	23.87	1562	Dodecanoic acid	$C_{12}H_{24}O_2$	0.51	0.33
30.	23.88	1563	Nerolidol	$C_{15}H_{26}O$	0.27	-
31.	24.52	1587	Spathulenol	$C_{15}H_{24}O$	0.37	0.06
32.	24.69	1594	Caryophyllene oxide	$C_{15}H_{24}O$	0.75	0.17
33.	25.69	1638	α-Copaen-8-ol	$C_{15}H_{24}O$	1.94	-
34.	27.21	1700	β-Sinensal	$C_{15}H_{22}O$	0.29	-
35.	28.52	1759	Tetradecanoic acid	$C_{14}H_{28}O_2$	0.45	0.25
36.	29.94	1823	Nootkatone	$C_{15}H_{22}O$	5.91	0.15
37.	30.64	1857	Umbelliferone	$C_9H_6O_3$	0.20	-
38.	30.96	1873	Platambin	$C_{15}H_{26}O_2$	0.2	0.08
39.	31.96	1919	(E,E)-Farnesyl acetone	$C_{18}H_{30}O$	0.38	-
40.	32.01	1921	Hexadecanoic acid, methyl ester	$C_{17}H_{34}O_2$	-	0.53
41.	32.98	1969	Hexadecanoic acid	$C_{16}H_{32}O_2$	3.42	10.77
42.	34.22	2045	Heptadecanoic acid	$C_{17}H_{34}O_2$	-	0.2
43.	35.08	2076	Xanthotoxin	$C_{12}H_8O_4$	0.19	0.27
44.	35.41	2098	Heneicosane	$C_{21}H_{44}$	0.41	1.48
45.	35.54	2099	(Z,Z)-9,12-Octadecenoic acid methyl ester	$C_{19}H_{34}O_2$	-	1.04
46.	35.62	2102	(Z)-9-Octadecenoic acid methyl ester	$C_{19}H_{36}O_2$	-	0.03
47.	36.53	2147	(Z)-9-Octadecenoic acid	$C_{18}H_{34}O_2$	2.74	20.79
48.	37.29	2194	Docosane	$C_{22}H_{46}$	0.60	1.98
49.	39.11	2296	Tricosane	$C_{23}H_{48}$	4.34	6.95
50.	40.77	2396	Tetracosane	$C_{24}H_{50}$	2.0	2.62
51.	41.96	2473	Pentacosanol	$C_{25}H_{50}O$	0.28	0.55
52.	42.28	2495	Pentacosane	$C_{25}H_{52}$	3.70	4.46
53.	43.61	2594	Hexacosane	$C_{26}H_{54}$	1.07	2.43
54.	44.45	2631	Auraptene	$C_{19}H_{22}O_3$	8.39	2.80
55.	44.81	2696	Heptacosane	$C_{27}H_{56}$	-	1.5
56.	45.88	2797	Octacosane	$C_{28}H_{58}$	-	0.21
57.	46.35	2833	Squalene	$C_{30}H_{50}$	2.56	0.18
58.	49.78	3000<	Vitamine E	$C_{29}H_{50}O_2$	1.69	-
59.	50.69	3000<	Tangeritin	$C_{20}H_{20}O_7$	1.05	-
60.	51.37	3000<	δ5-Ergostenol	$C_{28}H_{48}O$	3.25	2.14

61.	51.80	3000<	Stigmasterol	$C_{29}H_{48}O$	2.06	0.67
62.	52.71	3000<	γ-Sitosterol	$C_{29}H_{50}O$	5.08	-
63.	53.37	3000<	Nobilitin	$C_{21}H_{22}O_8$	0.31	-

[a)] retention indices relative to C_7-C_{30} n-alkanes calculated on Rtx-5MS capillary column.

[b)] supercritical CO_2 extract of fruit compounds tentatively identified based on retention index and elution order as well as the fragmentation pattern described in the literature.

[c)] relative peak area percentage (peak area relative to the total peak area %)

-[d)], not detected

Table 5. Chemical compounds identified from supercritical extract of immature phalsak variety

SN	RT	RI [a)]	Name [b)]	MF	Area% [c)]	
					Peel	Flesh
1.	8.86	1030	Sylvestrene	$C_{10}H_{16}$	4.24	- [d)]
2.	9.12	1039	Limonene	$C_{10}H_{16}$	7.98	8.03
3.	9.75	1061	γ-Terpinene	$C_{10}H_{16}$	4.86	3.28
4.	10.92	1098	Linalool	$C_{10}H_{18}O$	1.79	1.48
5.	13.71	1191	α-Terpineol	$C_{10}H_{18}O$	1.61	-
6.	14.07	1201	Decanal	$C_{10}H_{20}O$	0.72	-
7.	18.58	1361	Neryl acetate	$C_{12}H_{36}O_2$	1.05	-
8.	19.09	1378	Geranyl acetate	$C_{12}H_{36}O_2$	1.09	-
9.	19.46	1391	β-Elemene	$C_{15}H_{24}$	0.88	-
10.	19.80	1403	Decyl acetate	$C_{15}H_{24}$	0.4	-
11.	21.93	1485	Germacrene-D	$C_{15}H_{24}$	4.17	-
12.	22.31	1498	α-Selinene	$C_{15}H_{22}O$	1.67	-
13.	22.44	1504	Farnesene	$C_{15}H_{24}$	1.77	-
14.	22.61	1511	2,4-Di-tert-butylphenol	$C_{14}H_{22}O$	-	0.35
15.	22.97	1526	δ-Cadinene	$C_{15}H_{24}$	0.46	-
16.	23.62	1552	Elemol	$C_{15}H_{26}O$	0.31	-
17.	29.12	1786	Ethyl myristate	$C_{16}H_{32}O_2$	0.2	-
18.	31.97	1919	Methyl palmitate	$C_{17}H_{34}O_2$	-	0.27
19.	33.30	1984	Ethyl palmitate	$C_{18}H_{36}O_2$	0.26	-
20.	36.20	2135	Ethyl linoleate	$C_{20}H_{36}O_2$	-	2.80
21.	36.28	2139	Octadecanoic acid	$C_{18}H_{36}O_2$	-	1.17
22.	36.45	2148	Osthol	$C_{15}H_{16}O_3$	0.66	-
23.	37.22	2189	Docosane	$C_{22}H_{46}$	-	0.65
24.	37.96	2231	7-Methoxy-8-(2-formyl-2-methylpropyl)coumarin	$C_{15}H_{16}O_4$	1.68	-
25.	38.13	2241	Xanthotoxol	$C_{11}H_6O_4$	0.84	-
26.	38.31	2251	1,1,4,4-Tetramethyl-2-tetralone	$C_{14}H_{18}O$	20.86	-

27.	38.36	2253	Methyldocosane	$C_{23}H_{49}$	-	3.42
28.	39.02	2291	Tricosane	$C_{23}H_{48}$	-	5.37
29.	39.20	2300	7-Methoxy-8-(2-oxo-3-methylbutyl)coumarin	$C_{15}H_{16}O$	1.37	-
30.	40.09	2354	2-Methyltricosane	$C_{24}H_{52}$	-	0.79
31.	40.27	2364	9-Butyldocosane	$C_{26}H_{54}$	-	3.05
32.	40.70	2390	Tetracosane	$C_{24}H_{50}$	-	2.08
33.	41.67	2454	Methyltetracosane	$C_{25}H_{54}$	-	4.82
34.	42.22	2491	Pentacosane	CvH_{52}	-	5.94
35.	43.21	2565	3-Methylpentacosane	$C_{26}H_{54}$	-	2.83
36.	43.54	2590	Hexacosane	$C_{26}H_{54}$	-	0.98
37.	44.08	2633	Alloimperatorin	$C_{16}H_{14}O_4$	8.15	-
38.	44.31	2653	Auraptene	$C_{19}H_{22}O_3$	7.29	0.54
39.	44.32	2653	8-Methylhexacosane	$C_{27}H_{54}$	-	1.73
40.	44.76	2690	Heptacosane	$C_{27}H_{56}$	-	2.14
41.	45.59	2798	Octacosane	$C_{28}H_{58}$	-	1.03
42.	46.30	2829	Squalene	$C_{30}H_{50}$	-	1.26
43.	47.63	3000	Triacontane	$C_{30}H_{62}$	-	0.28
44.	48.70	3000<	γ-Tocopherol	$C_{28}H_{48}O_2$	0.73	-
45.	49.64	3000<	α-tocopherol	$C_{28}H_{48}O_2$	2.41	0.86
46.	50.57	3000<	4',5,6,7,8-Pentamethoxyflavone	$C_{20}H_{20}O_7$	1.78	-
47.	51.20	3000<	δ5-Ergostenol	$C_{28}H_{48}O$	1.87	9.6
48.	51.64	3000<	Stigmasterol	$C_{29}H_{48}O$	1.34	2.71
49.	52.52	3000<	γ-Sitosterol	$C_{29}H_{50}O$	4.38	16.65
50.	53.26	3000<	3',4',5,6,7,8-Hexamethoxyflavone	$C_{21}H_{22}O_8$	0.24	-

[a)] retention indices relative to C_7-C_{30} n-alkanes calculated on Rtx-5MS capillary column.

[b)] supercritical CO_2 extract of fruit compounds tentatively identified based on retention index and elution order as well as the fragmentation pattern described in the literature.

[c)] relative peak area percentage (peak area relative to the total peak area %)

-[d)], not detected

A

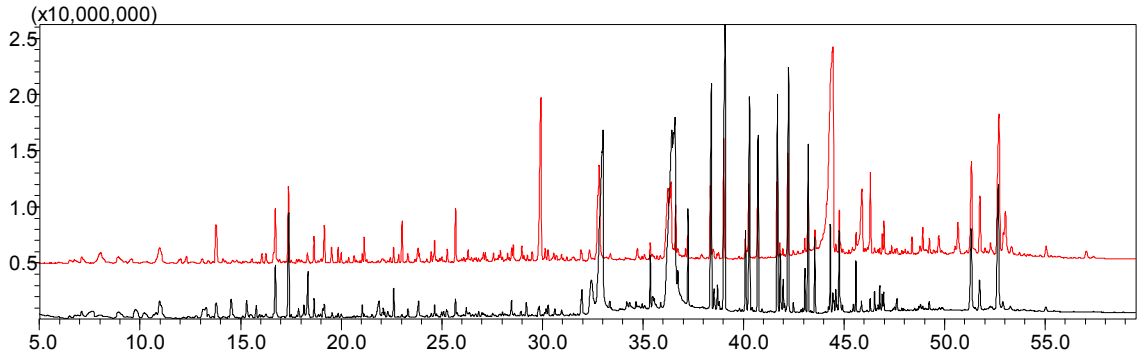

B

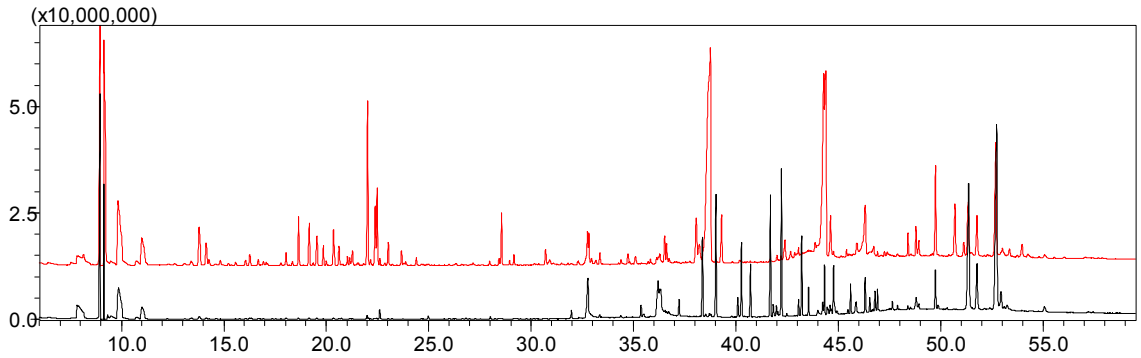

Figure. 8. GC-MS chromatogram of supercritical extract of phalsak varieties from Jeju, Korea. A: Mature *Citrus* SCEs, B: Immature *Citrus* SCEs. (Red : peel, Black : flesh)

Table 6. Chemical compounds identified from supercritical extract of mature yeagam variety

SN	RT	RI [a]	Name of the compound [b]	MF	Area% [c]	
					Peel	Flesh
1.	7.72	989	β-Myrcene	$C_{10}H_{16}$	0.10	0.18
2.	7.91	995	(*E,E*)-2,4-Heptadienal	$C_7H_{10}O$	0.21	0.16
3.	8.76	1027	p-Cymene	$C_{10}H_{14}$	1.30	0.6
4.	8.925	1033	Limonene	$C_{10}H_{16}$	21.87	10.62
5.	9.69	1059	2-Octenal	$C_8H_{14}O$	0.12	0.16
6.	10.995	1100	Linalool	$C_{10}H_{18}O$	8.32	0.94
7.	11.06	1102	Nonanal	$C_9H_{18}O$	- [d]	0.51
8.	12.02	1136	(*Z*)-Limonene oxide	$C_{10}H_{16}O$	0.22	0.22
9.	13.10	1172	Nonanool	$C_9H_{20}O$	0.33	-
10.	13.39	1180	4-Terpineol	$C_{10}H_{18}O$	0.40	0.39
11.	13.79	1193	α-Terpineol	$C_{10}H_{18}O$	2.03	0.28
12.	14.145	1204	Decanal	$C_{10}H_{20}O$	0.26	0.08
13.	14.27	1209	Octyl acetate	$C_{10}H_{20}O_2$	0.22	0.02
14.	14.64	1222	Carveol	$C_{10}H_{16}O$	0.18	0.22
15.	15.32	1246	Piperitenone oxide	$C_{10}H_{14}O_2$	-	0.53
16.	15.56	1255	α-Geraniol	$C_{10}H_{18}O$	0.18	-
17.	15.80	1264	(*E*)-2-Decenal	$C_{10}H_{18}O$	0.02	0.57
18.	16.295	1279	Perilla aldehyde	$C_{10}H_{14}O$	0.53	0.12
19.	16.795	1295	(*E,Z*)2,4-Decadienal	$C_{10}H_{16}O$	0.99	3.05
20.	16.96	1304	Thymol	$C_{10}H_{14}O$	0.29	-
21.	17.465	1320	(*E,E*)-2,4-Decadienal	$C_{10}H_{16}O$	0.87	4.82
22.	18.03	1341	δ-Elemene	$C_{15}H_{24}$	0.58	-
23.	18.68	1367	2-Undecenal	$C_{11}H_{20}O$	-	0.60
24.	18.695	1365	Neryl acetate	$C_{12}H_{20}O_2$	0.82	-
25.	19.225	1383	Geranyl acetate	$C_{12}H_{20}O_2$	2.08	-
26.	19.54	1398	Tetradecane	$C_{14}H_{30}$	-	0.14
27.	19.575	1395	β-Elemene	$C_{15}H_{24}$	0.76	-
28.	19.89	1406	Decyl acetate	$C_{12}H_{24}O_2$	0.56	0.06

29.	20.045	1412	Perillyl acetate	$C_{12}H_{18}O_2$	0.48	0.07
30.	20.415	1428	β-Caryophyllene	$C_{15}H_{24}$	0.66	0.07
31.	20.66	1435	α-Himachalene	$C_{15}H_{24}$	0.62	-
32.	20.81	1443	α-Guaiene	$C_{15}H_{24}$	0.19	-
33.	21.06	1452	(*E*)-Geranylacetone	$C_{13}H_{22}O$	-	0.10
34.	21.19	1459	β-Farnesene	$C_{15}H_{24}$	1.79	0.05
35.	21.325	1462	α-Humulene	$C_{15}H_{24}$	0.37	-
36.	21.68	1475	(E)-2-Dodecenal	$C_{12}H_{22}O$	-	0.19
37.	22.00	1487	Germacrene-D	$C_{15}H_{24}$	0.43	-
38.	22.18	1493	Farnesene	$C_{15}H_{24}$	-	0.13
39.	22.44	1503	α-Muurolene	$C_{15}H_{24}$	0.12	-
40.	22.62	1512	α-Chamigrene	$C_{15}H_{24}$	0.24	-
41.	22.67	1513	2,4-Di-tert-butylphenol	$C_{14}H_{22}O$	-	0.18
42.	23.07	1530	δ-Cadinene	$C_{15}H_{24}$	1.15	0.06
43.	23.68	1555	Elemol	$C_{15}H_{26}O$	0.16	-
44.	23.94	1565	Dodecanoic acid	$C_{12}H_{24}O_2$	-	0.41
45.	23.95	1565	(E)-Nerolidol	$C_{15}H_{26}O$	0.7	-
46.	24.545	1588	Spathulenol	$C_{15}H_{24}O$	0.66	0.06
47.	24.7	1594	Caryophyllene oxide	$C_{15}H_{24}O$	1.42	0.16
48.	27.26	1702	β-Sinensal	$C_{15}H_{22}O$	1.63	-
49.	27.835	1729	isospathulenol	$C_{15}H_{24}O$	0.58	-
50.	28.59	1763	Tetradecanoic acid	$C_{14}H_{28}O_2$	0.76	0.32
51.	29.905	1822	Nootkatone	$C_{15}H_{22}O$	1.03	0.14
52.	30.64	1857	Pentadecanoic acid	$C_{15}H_{30}O_2$	0.49	0.09
53.	31.04	1875	Platambin	$C_{15}H_{26}O_2$	0.92	-
54.	32.025	1922	Pentadecanoic acid methyl ester	$C_{16}H_{32}O_2$	-	0.73
55.	33.015	1971	Hexadecanoic acid	$C_{16}H_{32}O_2$	2.05	9.36
56.	33.4	1989	Hexadecanoic acid, ethyl ester	$C_{17}H_{34}O_2$	0.38	0.32
57.	35.36	2093	(Z,Z)-9,12- Octadecanoic acid methyl ester	$C_{19}H_{34}O_2$	0.16	-
58.	36.425	2150	(Z,Z)-9,12- Octadecanoic acid ethyl ester	$C_{20}H_{36}O_2$	1.2	15.33
59.	36.63	2160	(Z)-9-Octadecanoic acid ethyl ester	$C_{20}H_{38}O_2$	0.48	0.80
60.	37.28	2194	Docosane	$C_{22}H_{46}$	0.33	1.00

61.	39.085	2295	Tricosane	$C_{23}H_{48}$	0.10	4.08
62.	40.13	2356	2-Methyl tricosane	$C_{24}H_{50}$	0.51	1.03
63.	40.755	2393	Tetracosane	$C_{24}H_{50}$	0.82	1.98
64.	42.27	2494	Pentacosane	$C_{25}H_{52}$	0.16	3.53
65.	43.25	2568	Hexacosane	$C_{26}H_{54}$	0.47	2.39
66.	44.805	2696	Heptacosane	$C_{27}H_{56}$	0.20	1.98
67.	45.88	2798	Octacosane	$C_{28}H_{58}$	0.09	0.43
68.	46.375	2833	Squalene	$C_{30}H_{50}$	1.91	0.35
69.	50.8	3000<	Tangeritin	$C_{20}H_{20}O_7$	3.15	0.91
70.	51.41	3000<	δ5-Ergostenol	$C_{28}H_{48}O$	1.03	1.23
71.	51.845	3000<	Stigmasterol	$C_{29}H_{48}O$	1.54	0.58
72.	52.82	3000<	γ-Sitosterol	$C_{29}H_{50}O$	3.96	3.28
73.	53.5	3000<	Nobilitin	$C_{21}H_{22}O_8$	1.82	-
74.	55.15	3000<	Cycloartenol	$C_{30}H_{50}O$	0.27	-

[a)] retention indices relative to C_7-C_{30} n-alkanes calculated on Rtx-5MS capillary column.

[b)] supercritical CO_2 extract of fruit compounds tentatively identified based on retention index and elution order as well as the fragmentation pattern described in the literature.

[c)] relative peak area percentage (peak area relative to the total peak area %)

-[d)], not detected

Table 7. Chemical compounds identified from supercritical extract of immature yeagam variety

SN	RT	RI [a]	Name [b]	MF	Area% [c]	
					Peel	Flesh
1.	8.97	1034	Limonene	$C_{10}H_{16}$	22.19	3.6
2.	11.00	1101	Linalool	$C_{10}H_{18}O$	11.23	1.42
3.	13.78	1193	α-Terpineol	$C_{10}H_{18}O$	1.60	- [d]
4.	14.13	1204	Decanal	$C_{10}H_{20}O$	0.48	-
5.	16.26	1278	Perillal	$C_{10}H_{14}O$	0.29	-
6.	18.04	1341	δ-Elemene	$C_{15}H_{24}$	5.02	0.31
7.	18.62	1362	Limonene oxide	$C_{10}H_{16}O$	-	0.53
8.	18.64	1363	Neryl acetate	$C_{12}H_{20}O_2$	0.38	-
9.	19.16	1381	Geranyl acetate	$C^{12}H_{20}O_2$	1.13	-
10.	19.55	1394	β-Elemene	$C_{15}H_{24}$	1.55	-
11.	20.36	1426	β-Caryophyllen	$C_{15}H_{24}$	1.61	-
12.	21.14	1456	Nerolidol	$C_{15}H_{26}O$	1.17	-
13.	21.28	1461	α-Humulene	$C_{15}H_{24}$	0.72	-
14.	22.01	1488	Germacrene-D	$C_{15}H_{24}$	4.46	0.44
15.	22.40	1502	bicyclogermacrene	$C_{15}H_{24}$	0.35	-
16.	22.61	1511	2,4-Di-tert-butylphenol	$C_{14}H_2O$	-	0.77
17.	23.02	1528	δ-Cadinene	$C_{15}H_{24}$	0.92	-
18.	23.67	1555	Elemol	$C_{15}H_{26}O$	1.06	-
19.	23.88	1563	Nerolidol	$C_{15}H_{26}O$	0.24	-
20.	24.98	1606	4-(2,2,3,3-tetramethylbutyl)-phenol	$C14H_2O$	-	0.27
21.	27.17	1699	β-Sinensal	$C_{15}H_{22}O$	1.31	-
22.	28.45	1757	α-Sinensal	$C_{15}H_{22}O$	2.66	-
23.	29.16	1788	Ethyl myristate	$C_{16}H_{32}O_2$	0.29	-
24.	31.97	1919	Methyl palmitate	$C_{17}H_{34}O_2$	-	0.22
25.	32.78	1960	Hexadecanoic acid	$C_{16}H_{32}O_2$	-	4.21
26.	33.34	1987	Ethyl palmitate	$C_{18}H_{36}O_2$	0.36	-
27.	35.36	2098	Heneicosane	$C_{21}H_{44}$	-	0.62
28.	36.16	2133	Ethyl linoleate	$C_{20}H_{36}O_2$	-	2.52

29.	36.25	2138	Octadecanoic acid	$C_{18}H_{36}O_2$	-	2.58
30.	37.22	2189	Docosane	$C_{22}H_{46}$	-	1.52
31.	38.35	2253	3-Methyldocosane	$C_{23}H_{49}$	-	4.89
32.	39.05	2298	Tricosane	$C_{23}H_{48}$	-	12.10
33.	40.69	2389	Tetracosane	$C_{24}H_{50}$	-	3.89
34.	41.66	2454	2-Methyltetracosane	$C_{25}H_{52}$	-	6.59
35.	41.96	2474	Pentacosanol	$C_{15}H_{32}O$	-	0.44
36.	42.19	2490	Pentacosane	$C_{25}H_{52}$	-	9.11
37.	43.53	2589	Hexacosane	$C_{26}H_{54}$	-	1.46
38.	44.75	2699	Heptacosane	$C_{27}H_{56}$	-	2.51
39.	46.30	2790	Squalene	$C_{30}H_{50}$	1.19	0.67
40.	48.78	3000<	γ-Tocopherol	$C_{28}H_{48}O_2$	1.33	-
41.	49.75	3000<	α-Tocopherol	$C_{28}H_{48}O_2$	4.24	-
42.	50.73	3000<	4',5,6,7,8-Pentamethoxyflavone	$C_{20}H_{20}O_7$	4.68	0.5
43.	51.34	3000<	δ5-Ergostenol	$C_{28}H_{48}O$	2.18	5.54
44.	51.78	3000<	Stigmasterol	$C_{29}H_{48}O$	2.86	2.05
45.	52.73	3000<	γ-Sitosterol	$C_{29}H_{50}O$	9.12	11.72
46.	53.40	3000<	3',4',5,6,7,8-Hexamethoxyflavone	$C_{21}H_{22}O_8$	1.59	0.3

[a)] retention indices relative to C_7-C_{30} n-alkanes calculated on Rtx-5MS capillary column.

[b)] supercritical CO_2 extract of fruit compounds tentatively identified based on retention index and elution order as well as the fragmentation pattern described in the literature.

[c)] relative peak area percentage (peak area relative to the total peak area %)

-[d)], not detected

A

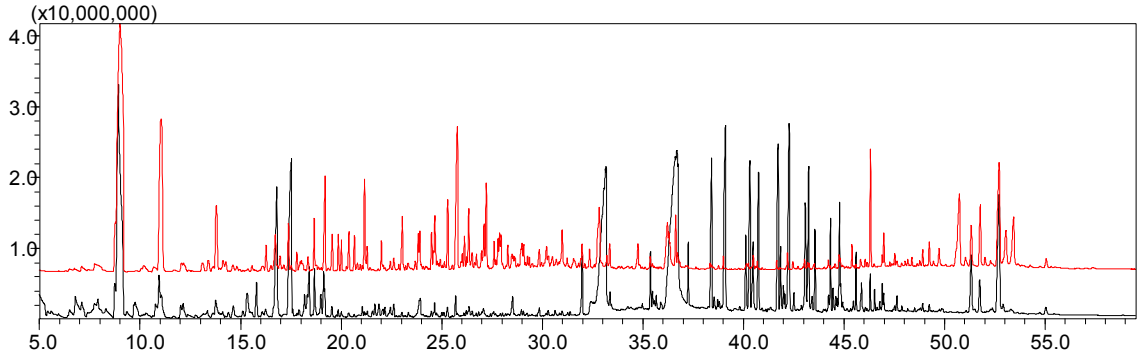

B

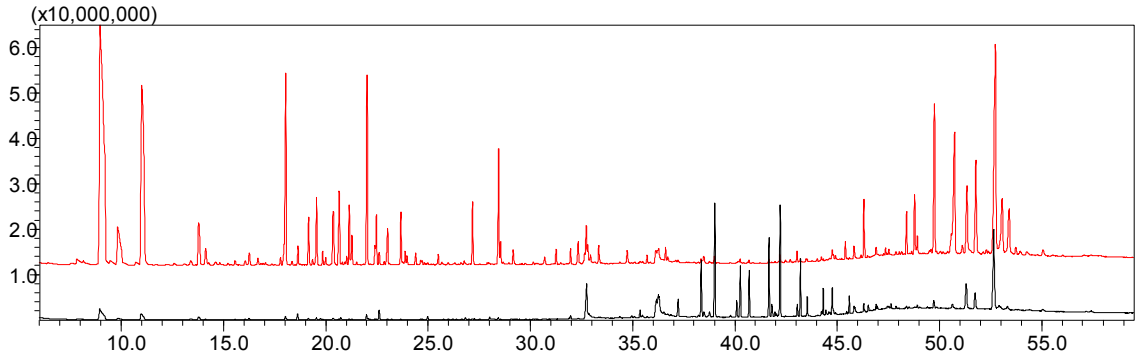

Figure. 9. GC-MS chromatogram of supercritical extract of yeagam varieties from Jeju, Korea. A: Mature *Citrus* SCEs, B: Immature *Citrus* SCEs. (Red : peel, Black : flesh)

4.3. Cytotoxic effect of auraptene

Since both immature and mature fruit fraction showed strong anticancer effect, any of the common compound, either individually or in synergistic cooperation with the other compound, could be the anticancer candidate. Since cytotoxic effect and abundance of auraptene is significantly greater in the peel fraction than in the flesh fraction of both the mature and immature fruits, we presume that auraptene is highly likely to be the most potent anticancer candidate present in the phalsak (*Citrus hassaku* Hort ex Tanaka) fruit. For this reason, we have studied rest of the anticancer effects taking auraptene as a possible therapeutic candidate in the treatment of human gastric cancer. Although, auraptene has previously been reported to induce chemopreventive agent against various types of cancers such as liver, skin, tongue, esophagus and colon in rodent models (Curini *et al*., 2006), its effect in human gastric cancer is poorly reported, this is also substantiated our interest in anticancer effect of auraptene. As shown in Figure. 10, auraptene reduced the viability of all type of tested gastric cancer cells in a dose-dependent manner. Among them, SNU-1 was the most sensitive with IC_{50} value $\leq$ 25 μM. In the contrast, auraptene did not pose cytotoxic effect against non cancer cell lines 293T. Therefore, auraptene has high potentiality to treat gastric cancer cells without harming normal cells.

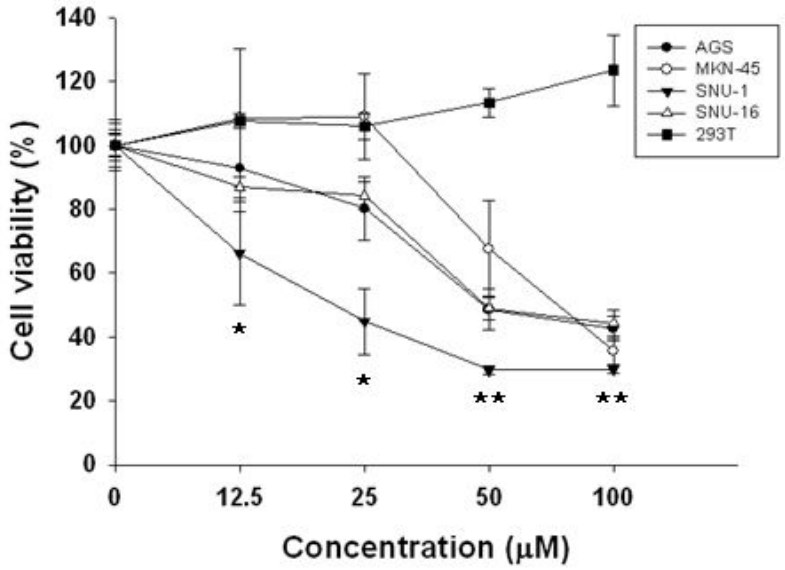

Figure. 10. Cell growth inhibition by auraptene. Viability was determined on the basis of MTT reduction assay against various cancer cell lines and a non-cancer cell line after treating with shown concentration of auraptene for 48 h. (* $p<0.05$, ** $p<0.01$).

4. 4. Effect of Auraptene on cell morphology, cell cycle distribution and $\Delta\Psi m$

Morphological changes such as cell shrinkage, blebbing, condensation, and fragmentation of chromatin are associated with apoptotic cell death. To evaluate the effect of auraptene on proliferation and to characterize auraptene-induced apoptosis, SNU-1 cells were treated with or without various concentrations of auraptene and stained with Hoechst 33342 and then observed under fluorescence microscopy. As shown in Figure. 11(A), after treatment with 25, 50 and 100 μM auraptene, SNU-1 cells showed morphological changes including condensed and fragmented chromatin with dose dependently increased apoptotic bodies (arrows). Cell cycle regulation is the major regulatory mechanism of cell growth. Many cytotoxic agents arrest the cell cycle at the G1, S, or G2/M phases, cause cells to accumulate in the sub-G1 phase, and then induce apoptotic cell death. In this study, signs of apoptosis were indicated by the increased sub-G1 SNU-1 cells after auraptene treatment in a concentration-dependent manner. The sub-G1 population was increased from 4.8% (0 μM) to 23.5% (100 μM) (Fig. 11B).

In addition, low concentration of auraptene (50 μM) caused a significant increase in the G1 population (from 61.3% to 75.4%). This data suggest that auraptene inhibits SNU-1 cell proliferation by inducing G1 cell cycle arrest at relatively lower concentrations and causing the accumulation of sub-G1 cells at higher concentrations. As depicted in Figure. 11(C) auraptene caused decrease in the $\Delta\Psi m$ in concentration dependent manner; from 85.66% at control to 12.13% at 100 μM. From these results it is clear that auraptene caused apoptotic cell death in SNU-1.

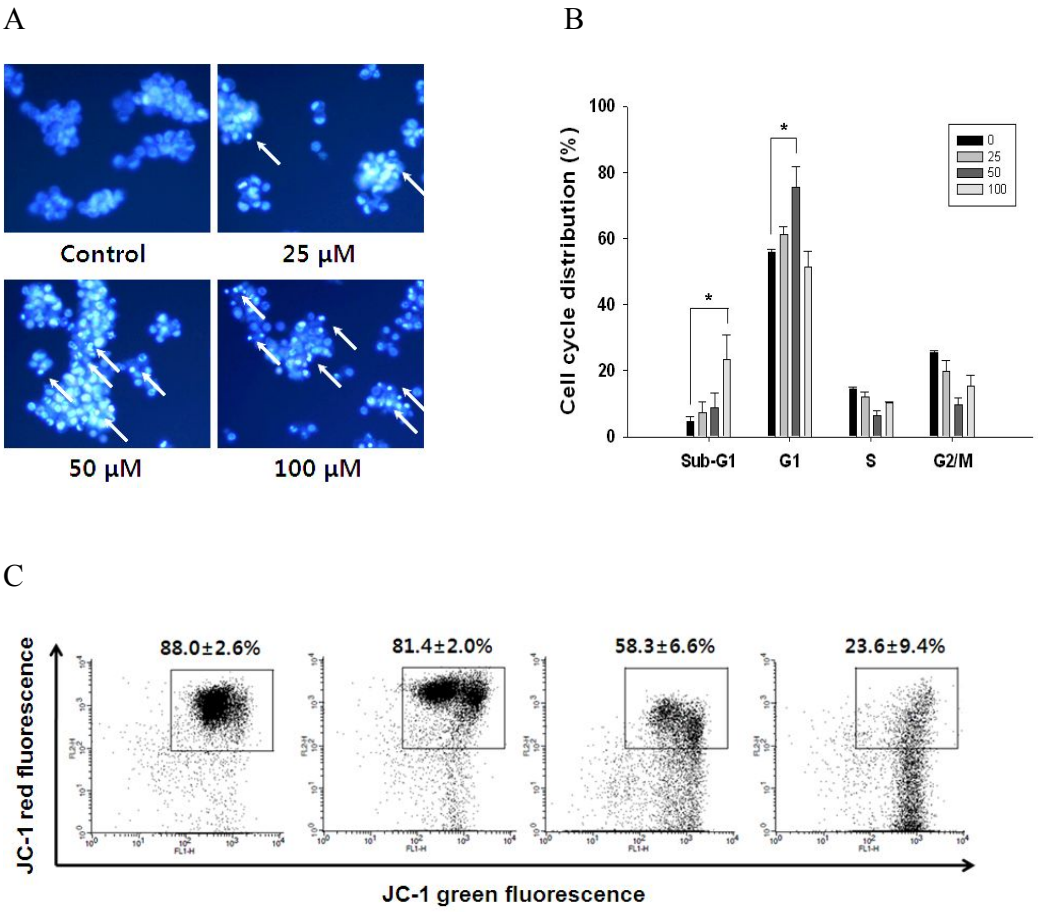

Figure. 11. Nuclear Hoechst 33342 staining, cell cycle analysis and determination of mitochondrial membrane potential. (A) Cells were treated with the indicated concentration of auraptene (25-100 μM) for 24 h and then stained with Hoechst 33342. Stained cells were visualized under a fluorescence microscope. (B) Analyzed for cell-cycle distribution using propidium iodide and a flow cytometric system. (C) Mitochondrial membrane potential was determined by FACScaliber after treated with given doses of auraptene.

4. 5. Effects of auraptene on the regulation of apoptosis-related proteins

Apoptosis is regulated by various types of modulators, among them caspases have been studied in more detail (Ulukaya *et al*., 2011). To determine the mechanism of auraptene-induced apoptosis, the regulation of apoptotic proteins were examined by western blotting after auraptene treatment. The protein level of effector caspases, caspase-7 and caspase-3, were found reduced dose dependently. Further, the level of proteolytically cleaved PARP was found increased by dose dependently (Fig. 12). The prevention of cancer is largely dependent on tumor suppressor protein p53. Removal of excess, damaged or infected cells through p53-induced apoptosis is crucial for the regulation of cell proliferation in multicellular organisms. Cellular stress can trigger p53 which induces cell cycle arrest or apoptosis. The choice between apoptosis or cell cycle arrest is influenced by many factors such as type of cell and stress, action of p53 co-activators (Haupt *et al*., 2003). As illustrated in Fig. 12, auraptene dose dependently induced the expression of p53. Further, when DNA damage occur, activated p53 halts the progression of cell cycle in G1 phase to provide time for DNA repair (Ulukaya *et al*., 2011). Here, auraptene caused dose dependent down regulation of cyclin D1 which indicates that auraptene induced cell cycle arrest in SNU-1. In summary, auraptene caused activation of p53 which then caused cell cycle arrest and/or apoptosis via various related proteins.

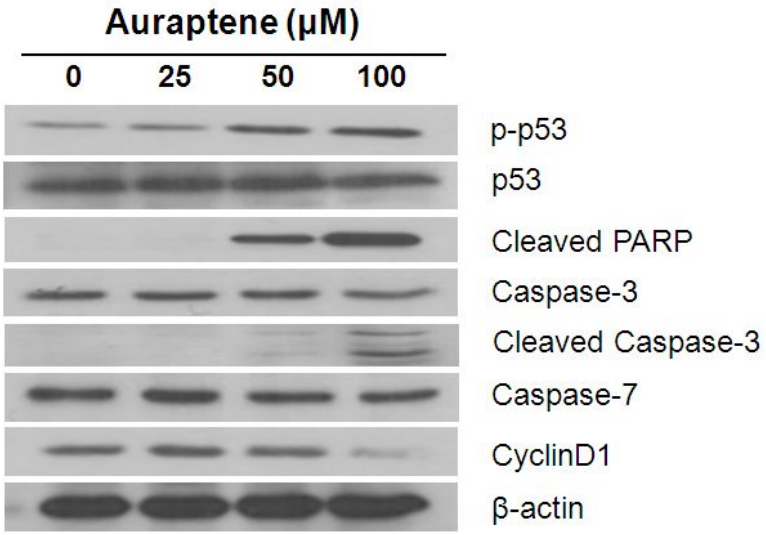

Figure. 12. Western blot analysis of apoptosis and cell cycle related protein expression. Cells were lysed after incubation with different concentrations of auraptene (25-100 μM). After 24 h, cell lysates were subjected to western blotting as mentioned in the method. β-actin was used as an internal control.

4. 6. Auraptene induces negative feedback activation of Akt signaling by inhibition of mTOR

The PI3K/Akt/mTOR pathway is an intracellular signalling pathway important in apoptosis. Therefore, we confirmed that whether auraptene induced apoptosis through the PI3K/Akt/mTOR signaling by western blotting. As shown in Fig. 13 (A), phospho-Akt level was increased, whereas phospho-mTOR was decreased. However, down-regulation of p-p70S6K and up-regulation of p-4EBP1, downstream of mTOR proteins, means auraptene has effect of mTOR inhibition, like rapamycin (mTOR inhibitor). Therefore, we performed that whether rapamycin (mTOR inhibitor) induced also negative feedback activation of Akt in SNU-1 cells. As a result, rapamycin was very similar to auraptene effects (Fig. 13B). We suggesting that auraptene could induce negative feedback activation of Akt in SNU-1 based on accumulation of phosphorylated Akt, no sign of mTOR and 4EBP1, one of the downstream proteins of mTOR.

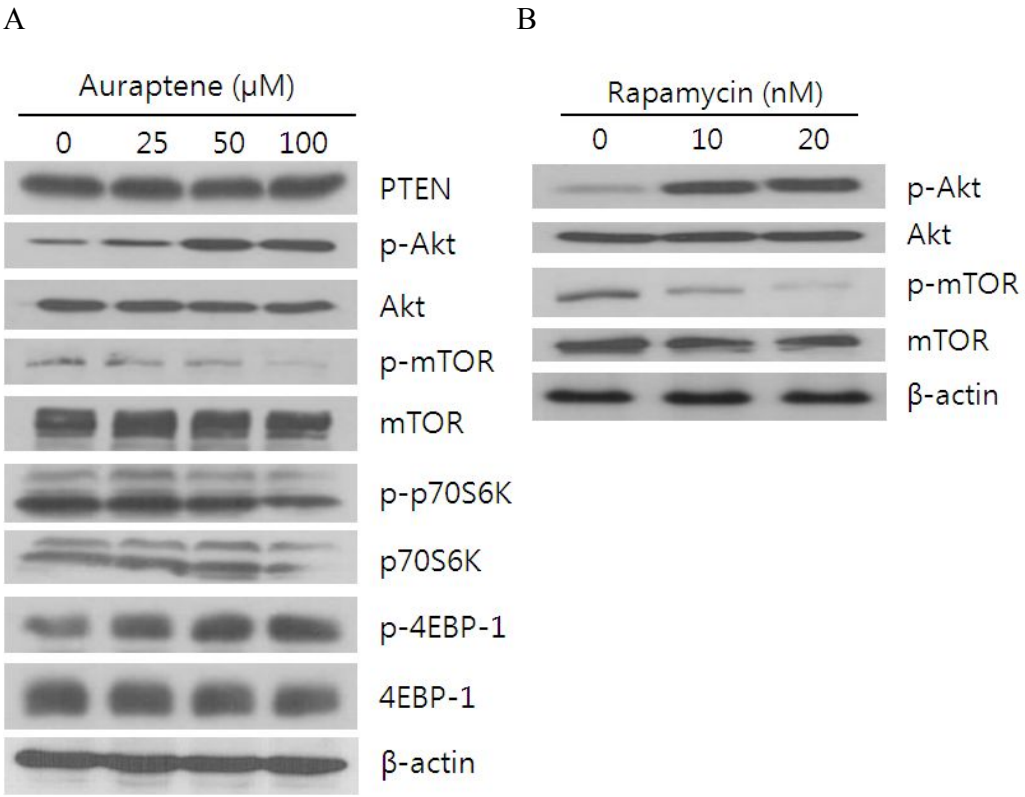

Figure. 13. Inhibition of mammalian target of rapamycin (mTOR) signaling by auraptene leads to an increase of Akt phosphorylation in SNU-1 cells. (A) Western blotting for Akt/mTOR related proteins using auraptene-treated lysates from SNU-1 cells. (B) Cells were treated with repamycin for 24 h in SNU-1 cells.

5. DISCUSSION

Supercritical Extraction (SCE) is the process of separating one component (the extractant) from another (the matrix) using supercritical fluids as the extracting solvent. In this study, Jeju *Citrus* extraction conditions for Supercritical carbon dioxide were above the critical temperature of 31°C and critical pressure of 74 bar. We determined the cytotoxic effect of SCE from peel and flesh of Jeju *Citrus* (dangyuja, phalsak, and yeagam). As a result, immature phalsak peel SCE induced significantly inhibition of cell viability in AGS, compared to other peel SCEs.

In most of the studies of volatile composition of *Citrus* fruits obtained by different conventional methods of extractions, limonene was found in a proportion of >94.8% (Kamal *et al*., 2011; Patil *et al*., 2009). However, in the present study limonene was found to be extremely low levels in dangyuja, phalsak and yeagam. The discrepancy of results reported in the present work can be attributed to the sample type and chemical complexity of the supercritical extracts as well as also due to the geographical origin of samples. We analysis mature and immature SCEs and compare with which compounds contribute to the cell death. Among the components of phalsak SCEs, auraptene was found in both peel and flesh SCEs but the proportions was a great difference between peel and flesh. Next, we performed effect of auraptene by MTT, cell cycle analysis, JC-1 staining, Hoechst33342 staining, and western blot, whether induced cell death or not. As a result, auraptene reduced the viability of tested gastric cancer cell lines, SNU-1 was the most sensitive. Auraptene, also, indicated that cell cycle arrest (low concentration), increase of sub-G1 phase, disturbed mitochondria membrane potential, and activation of apoptosis related proteins. Decrease in $\Delta\Psi m$ is often regarded as a sign of apoptosis. It has been suggested that chemically induced apoptosis is often associated with the loss of $\Delta\Psi m$ as a consequence of the leakiness of the inner mitochondrial membrane (Sun *et al*., 1999). These results suggest that auraptene induced cell death through the caspase

dependent apoptosis. But we noticed that auraptene also induced phosphorylation of Akt, in only SNU-1, not AGS and SNU-16 (data not shown). However, down-regulation of p-p70S6K and up-regulation of p-4EBP1, downstream of mTOR proteins, means auraptene has effect of mTOR inhibition, like rapamycin (mTOR inhibitor). Therefore we suggest that auraptene could induce apoptosis through the negative feedback activation of Akt in SNU-1 and down-regulation of mTOR.

PART IV

Anticancer activity of Nobiletin and its Mechanism in p53-Mutated SNU-16 Human Gastric Cancer cells

1. Nobiletin Potentiates the Effects of the Anticancer Drug 5-Fluorouracil

2. Nobiletin Induces Endoplasmic Reticulum Stress-Mediated Autophagy/Apoptosis

1. ABSTRACT

Nobiletin is a typical polymethoxyl flavone from *Citrus* fruits that has anticancer properties, but the molecular mechanism of its inhibitory effects on the growth of p53-mutated SNU-16 human gastric cancer cells has not been explored. In this study, nobiletin was found to be more effective at inhibiting the proliferation of SNU-16 cells than the flavonoids baicalein, quercetin, and hesperetin. Nobiletin induced the death of SNU-16 cells through apoptosis, as evidenced by the increased cell population in the sub-G1 phase, the appearance of fragmented nuclei, an increase in the Bax/Bcl-2 ratio, the proteolytic activation of caspase-9, an increase in caspase-3 activity, and the degradation of poly (ADP-ribose) polymerase (PARP) protein. In addition, the combination of nobiletin plus the anticancer drug 5-fluorouracil (5-FU) reduced the viability of SNU-16 cells in a concentration-dependent manner and exhibited a synergistic anticancer effect (CI=0.47) when 5-FU was used at relatively low concentrations. The expression of p53 protein increased after treatment with 5-FU, but not nobiletin, whereas the expression of $p21^{WAF1/CIP1}$ protein increased after treatment with nobiletin, but not 5-FU. The cellular responses to nobiletin and 5-FU occurred through different pathways. The results of this study suggest that the potential application of nobiletin to the enhancement of 5-FU efficiency in p53 mutant tumors. In addition, 2-DE-gel electrophoresis of SNU-16 cells induced with nobiletin showed that total, marked 17 spots were successfully identified, 9 proteins are identified as up-regulated and 8 as down-regulated. We assessed the peptide mass fingerprints (PMF) of 17 spots and compared them with the theoretical PMF of identified proteins. These results suggest that nobiletin was enhanced apoptosis by the combination treatment with fluorouracil. Moreover, nobiletin was regulated rho GDP dissociation inhibitor 1, 78 kDa glucose-regulated protein (GRP78), TXNDC5 and comm domain containing protein 9, eukaryotic translation initiation factor 4E,

peroxiredoxin3, -6 and so on. GRP78 protein increase by nobiletin in SNU-16 cells, but not AGS and SNU-1, and determined the level of another ER stress-related proteins caspase-4 and the level of LC3II protein as an autophagy marker. Furthermore, when nobiletin-induced autophagy was blocked by chloroquine treatment, the anti-proliferaive effect, sub-G1 phase, and the level of cleaved PARP were increased. Therefore, autophagy induced by nobiletin has a role in cell survival. Our findings indicate that SNU-16 cells are more sensitive to nobiletin than another phytochemicals, and the effect was associated with a high sensitivity to ER stress-mediated apoptosis and autophagy. To the best of our knowledge, this study provides the first evidence for an ER stress response in nobiletin-treated p53-mutated SNU-16 human gastric cancer cells.

2. INTRODUCTION

Nobiletin, a compound isolated from *Citrus* fruits, is a polymethoxylated flavone derivative shown to have antiinflammatory, antitumor, and neuroprotective properties. Nobiletin has the typical flavonoid structure and contains 6 methoxyl groups (Fig. 14) (Manthey and Guthrie, 2002). Recently, nobiletin was shown to down-regulated matrix metalloproteinase-7 (matrilysin) expression and to inhibits the DNA-binding activity of NF-κB and ROS production in LPS-activated RAW 264.7 cells (Choi *et al*., 2007; Kawabata *et al*., 2005) and to suppresses invasion and migration through the FAK/PI3K/Akt and small GTPase signals in human gastric adenocarcinoma AGS cells (Lee *et al*., 2011). In lung cancer cell, A549, also nobiletin shown that induce p53-mediated cell cycle arrest and apoptosis via modulated the Bax/Bcl-2 protein ratio (Luo *et al*., 2008). Although it is quite clear that nobiletin may inhibit the growth of various cancers by inducing cancer cells toward apoptosis or metastasis, the precise impact of nobiletin on cellular proteins is still uncertain. Thus, we investigated the effects and mechanisms by which nobiletin suppresses or enhances the apoptosis and growth inhibition target proteins of SNU-16 cells.

The endoplasmic reticulum (ER) performs several functions including protein folding and trafficking and the regulation of the intracellular calcium concentration. Upon disruption of the ER functions by accumulation of unfolded/misfolded proteins in the ER, cells trigger the unfolded protein response (UPR) as a self-protective mechanism (Schro¨der and Kaufman 2005). Under normal conditions, the ER stress sensors, IRE1, PERK, and ATF6, reside with binding to Bip/GRP78 but release from Bip/GRP78 by ER stress and transfer downstream signals to the cytoplasm. IRE1 activates the downstream target, X-box-binding protein-1 (XBP1), and activates several UPR target genes. PERK phosphorylates eIF2 to block translation. Activation of ATF6 increases transcription of ER chaperones, including BiP/GRP78, which is

involved in stress mitigation. In addition, the UPR activates the ER-associated degradation (ERAD) system. In this pathway, misfolded/unfolded proteins are translocated from the ER lumen to the cytosol and are then degraded by the ubiquitin proteosome pathway (Meusser *et al*., 2005). As a consequence, the UPR contributes to the reduction of ER overload and functions to protect cells against ER stress. However, if the ER functions are severely affected, cells are removed by apoptosis. ER stress-mediated apoptosis is triggered by the activation of ER membrane resident caspase-12 (mice) and caspase-4 (humans) and induction of Chop (Morishima *et al*., 2002; Rao *et al*., 2002; Oyadomari and Mori, 2004). Autophagy is a cellular defense mechanism that occurs through degradation and recycling of cytoplasmic constituents. Starvation-induced autophagy is known to have an important role in cell survival, whereas excessive autophagy triggers cell death (Baehrecke, 2005; Codogno and Meijer, 2005). During autophagy, cytoplasmic constituents are sequestered into double-membrane vesicles (autophagosomes) that subsequently fuse with lysosomes to form autolysosomes and are eventually, degraded by lysosomal hydrolases. Autophagic cell death is thus characterized by the accumulation of vacuoles (Klionsky and Emr, 2000). Accumulating evidence has suggested that ER stress is linked to autophagy (Ogata *et al*., 2006; Yorimitsu *et al*., 2006). However, the cellular consequences of ER stress-mediated autophagy seem to vary depending on the cell type and stimulus. As relevant in pathogenesis, disruption of autophagy may be a cause of several neurodegenerative disorders such as Parkinson's disease, Huntington disease, and Alzheimer's disease (Kaufman, 2002). Under autophagy-deficient conditions, toxic proteins that accumulate in the ER can be effectively removed by autophagy (Teckman and Perlmutter, 2000; Fujita *et al*., 2007); suggesting that ER stress-induced autophagy may play an important role in cell protection. Furthermore, a recent study showed that autophagy induced by ER stress inducers mitigates ER stress and protects cells. In contrast, autophagy that was induced by the same chemicals contributed to cell death in non-transformed cells (Ding *et al*., 2007).

However, it is still unclear whether ER stress-mediated autophagy is involved in cell survival or cell death. In the present study, we investigated whether the distinct response to normal cells of nobiletin is associated with ER stress response and autophagy.

3. MATERIALS AND METHODS

3.1. Chemicals and reagents

Nobiletin, hesperetin, quercetin, baicalein, 5-FU, propidium iodide (PI), anti-β-actin antibody, and a caspase-3 assay kit were purchased from Sigma (St. Louis, MO, USA). Caspase-9 assay kit was purchased from BioVision (Mountain View, CA, USA). RPMI-1640 medium, trypsin/EDTA, fetal bovine serum (FBS), penicillin, streptomycin, Hoechst 33342, goat anti-rabbit IgG, and goat anti-mouse IgG secondary antibodies were obtained from Life Technologies Corp. (Carlsbad, CA, USA). Dimethyl sulfoxide (DMSO) and MTT were purchased from Amresco (Cleveland, OH, USA). Antibodies specific for caspase-9, caspase-7, caspase-3, $p21^{WAF1/CIP1}$, poly (ADP-ribose) polymerase (PARP), Bax and Bcl-2 were obtained from Cell Signaling Technology (Beverly, MA, USA).

3.2. Cell culture

AGS, MKN-45, SNU-1, and SNU-16 cells were maintained at 37℃ in a humidified atmosphere containing 5% CO_2 in RPMI-1640 medium containing 10% heat-inactivated FBS, 100 U/mL penicillin, and 100 μg/mL streptomycin. Exponentially growing cells were treated with various concentrations of the solvent fractions, as indicated.

3.3. Cell viability assay

The inhibition of cell growth was determined by a MTT assay. Gastric cancer cells of four types were seeded in 96-well culture plates (5×10^4 cells/mL). After incubation overnight, cells were treated with various concentrations of nobiletin and 5-FU for 48 h. Then, 0.1 mg of MTT was added to each well, and the cells were incubated at 37℃ for 4 h. The medium was removed, and 150 μL of DMSO was then

added to each well to dissolve the formazan crystals. The absorbance at 570 nm was measured using a microplate reader (Tecan, Salzburg, Austria).

3.4. Analysis of the effects of drug combinations

The combination index (CI) was determined by the Chou-Talalay method (Chou and Talalay, 1984) using CalcuSyn software (Biosoft, Ferguson, MO, USA) and was expressed as the average of the CI values obtained at three different combinations. CI values of <1, 1, and >1 were considered to indicate synergistic, additive, and antagonistic effects, respectively.

3.5. Cellular morphology and DNA fragmentation

SNU-16 cells were left untreated or treated with samples. After 24, the DNA-specific fluorescent dye Hoechst 33342 (10 μM) was added to each well and the plates were incubated for 10 min at 37°C. Stained cells were then observed under a fluorescence microscope (Olympus, Tokyo, Japan). Genomic DNA was extracted in extraction buffer [10 mM Tris (pH 8.0), 0.1 M EDTA]. Sodium dodecyl sulfate (0.5%) was then added and the resulting mixture was incubated overnight at 50°C with 0.5 μg/μL proteinase K. The mixture was then extracted in phenol:chloroform:isoamyl alcohol (25:24:1) and the DNA precipitated with 5 M sodium chloride and 2 volumes of absolute ethanol. Extracted DNA (15 μg) was electrophoresed on a 1.8% agarose gel containing 0.1 g/mL ethidium bromide and visualized under ultraviolet light.

3.6. Flow cytometric analysis

For cell cycle distribution analysis, cells (5×10^4 mL) were plated and left untreated or treated with samples for 24 or 48 h. After treatment, the cells were collected, fixed in 70% ethanol, washed in 2 mM EDTA in phosphate-buffered saline (PBS), resuspended in 1 mL of PBS containing 1 mg/mL RNase and 50 mg/mL PI,

and incubated at 37 ℃ in the dark for 30 min. DNA content was analyzed using a FACScan flow cytometer (BD Biosciences, San Jose, CA, USA). For each data file, data from 10,000 cells were collected. The population of cells in each cell cycle phase was determined using CellQuest software (BD Biosciences). The sub-G1 population showed apoptosis-associated chromatin degradation.

3.7. Western blot analysis

After treatment, cells were collected and washed with PBS. They were then lysed in lysis buffer [50 mM Tris-HCl (pH 7.5), 150 mM NaCl, 1% Nonidet P-40, 2 mM EDTA, 1 mM EGTA, 1 mM $NaVO_3$, 10 mM NaF, 1 mM DTT, 1 mM PMSF, 25 μg/mL aprotinin, 25 μg/mL leupeptin] and kept on ice for 30 min. The lysates were then centrifuged at 13,000 rpm at 4°C for 30 min. The resulting supernatants were stored at –70°C until use. Protein concentration was determined using a bicinchoninic acid (BCA) protein assay kit (Pierce, Rockford, IL, USA). Aliquots of the lysates containing 60–100 μg of protein were separated by 7.5-15% SDS-PAGE and transferred onto a polyvinylidene difluoride (PVDF) membrane (Bio-Rad, Hercules, CA, USA) using glycine transfer buffer [192 mM glycine, 25 mM Tris-HCl (pH 8.8), 20% (v/v) methanol]. After blocking with 5% nonfat dried milk, the membrane was incubated for 2 h with primary antibody and then 30 min with secondary antibody in milk containing Tris-buffered saline (TBS) and 0.1% Tween 20. All primary antibodies were used at a dilution of 1:1,000; HRP-conjugated goat anti-rabbit IgG (H+L) and HRP-conjugated goat anti-mouse IgG were used as secondary antibodies at a dilution of 1:5,000. The PVDF membrane was then exposed to X-ray film (AGFA, Mortsel, Belgium), and the protein bands were detected using a WEST-ZOL® plus Western Blot Detection System (iNtRON, Gyeonggi-do, Korea).

3.8. Caspase-9, -3 activity assay

Caspase-9, -3 activity was assayed using a commercially available kit (BioVision and Sigma, respectively) according to the manufacturer's protocol. Untreated and sample-treated SNU-16 cells were lysed in chilled lysis buffer. The protein concentration was measured using a BCA protein assay kit. All mixtures were incubated overnight at 37°C in a humidified environment, and the absorbance at 405 nm of ρ-nitroaniline (ρ-NA) released from the substrate was measured using a Sunrise microplate reader (Tecan Group, Ltd., Männedorf, Switzerland).

3.9. 2-D materials

Urea, Thiourea, CHAPS, DTT, Benzamidine, Bradford solution, Acrylamide, Iodoacetamide, Bis-acrylamide, SDS, acetonitrile, trifluoroacetic acid, α-cyano-4-hydroxycinnamic acid were purchased from Sigma-Aldrich(Electrophoresis grade, ACS reagents, Ultrapure). Pharmalyte (pH3.5-10) was from Amersham Biosciences and IPG DryStrips(pH4-10NL, 24cm) were Genomine Inc. Modified porcine trypsin (sequencing grade) was from Promega.

3. 10. Protein sample preparation

1) Cultured animal or bacterial cell pellets were washed twice with ice-cold PBS(in molecular cloning) and sonicated for 10 seconds by Sonoplus (Bandelin electronic, Germany), 2) in case of animal or plant tissues, they were homogenized directly by motor-driven homogenizer (PowerGen125, Fisher Scientific) in sample lysis solution composed with 7M urea, 2M thiourea containing 4% (w/v) 3-[(3-cholamidopropy) dimethyammonio]-1-propanesulfonate (CHAPS), 1% (w/v) dithiothreitol(DTT) and 2%(v/v) pharmalyte and 1mM benzamidine. (Freezing and thawing step for yeasts or bacilli samples was repeated five times for one day. Occasionally bead beater was used for lysis of rigid cells). Proteins were extracted for one hour at room temperature with vortexing. After centrifugation at 15,000 × g for one hour at 15°C, insoluble

material was discarded and soluble fraction was used for two-dimensional gel electrophoresis. Protein loading was normalized by BCA assay kit.

3. 11. 2D PAGE

IPG dry strips were equilibrated for 12-16 hours with 7 M urea, 2 M thiourea containing 2% 3-[(3-cholamidopropy) dimethyammonio]-1-propanesulfonate (CHAPS), 1% dithiothreitol (DTT), 1% pharmalyte and respectively loaded with 200 μg of sample. Isoelectric focusing (IEF) was performed at 20°C using a Multiphor II electrophoresis unit and EPS 3500 XL power supply (Amersham Biosciences) following manufacturer's instruction. For IEF, the voltage was linearly increased from 150 to 3,500V during 3 hours for sample entry followed by constant 3,500 V, with focusing complete after 96 kVh. Prior to the second dimension, strips were incubated for 10 minutes in equilibration buffer(50 mM Tris-HCl, pH 6.8 containing 6 M urea, 2% SDS and 30% glycerol), first with 1% DTT and second with 2.5% iodoacetamide. Equilibrated strips were inserted onto SDS-PAGE gels (20 x 24cm, 10-16%). SDS-PAGE was performed using Hoefer DALT 2D system (Amersham Biosciences) following manufacturer's instruction. 2D gels were run at 20°C for 1,700 Vh. And then 2D gels were silver stained as described by Oakley et al (Oakley *et al*., 1980) but fixing and sensitization step with glutaraldehyde was omitted.

3. 12. Image analysis

Quantitative analysis of digitized images was carried out using the PDQuest (version 7.0, BioRad) software according to the protocols provided by the manufacturer. Quantity of each spot was normalized by total valid spot intensity. Protein spots were selected for the significant expression variation deviated over two fold in its expression level compared with control or normal sample.

3.13. Peptide Mass Fingerprinting (PMF)

For protein identification by peptide mass fingerprinting, protein spots were excised, digested with trypsin (Promega, Madison, WI), mixed with α-cyano-4-hydroxycinnamic acid in 50% acetonitrile /0.1% TFA, and subjected to MALDI-TOF analysis (Ettan MALDI-TOF Pro, Amersham Biosciences, Piscataway, NJ) as described Fernandez J *et al* (Electrophoresis 19: 1036-1045). Spectra were collected from 350 shots per spectrum over m/z range 600-3000 and calibrated by two point internal calibration using Trypsin auto-digestion peaks (m/z 842.5099, 2211.1046). Peak list was generated using Ettan MALDI-TOF Pro Evaluation Module (version 2.0.16). Threshold used for peak-picking was as follows: 5,000 for minimum resolution of monoisotopic mass, 2.5 for S/N. The search program MASCOT, developed by The Matrixscience (http://www.matrixscience.com), was used for protein identification by peptide mass fingerprinting. The following parameters were used for the database search: trypsin as the cleaving enzyme, a maximum of one missed cleavage, iodoacetamide (Cys) as a complete modification, oxidation (Met) as a partial modification, monoisotopic masses, and a mass tolerance of ± 0.1 Da. PMF acceptance criteria is probability scoring.

3.14. Statistical analysis

All experiments were repeated at least three times. Data are expressed as the mean±S.D. Statistical analysis was performed by analysis of variance (ANOVA). Values of $P<0.05$ were considered to be statistically significant.

4. RESULTS

4.1. Nobiletin inhibits the proliferation of SNU-16 cells

To investigate the cytotoxic effects of various flavonoids (Fig. 14) on p53-mutant SNU-16, human gastric cancer cell line, MTT assays were conducted. First, SNU-16 human gastric cancer cells were incubated with hesperetin (a flavonone), quercetin (a flavonol), baicalein (a flavone), and nobiletin (a flavone) for 48 h. As shown in Figure. 15(A), nobiletin reduced the viability of SNU-16 cells in a dose-dependent manner and had the highest cytotoxicity among the flavonoids. Then, four kinds of gastric cancer cells were exposed to various concentrations (12.5-200 μM) of nobiletin for 48 h. SNU-16 was most susceptible to nobiletin treatment among the tested gastric cancer cell lines (Fig. 15B). SNU-16 cells treated with 50 μM nobiletin for 48 h had 41.65% viability compared to untreated cells.

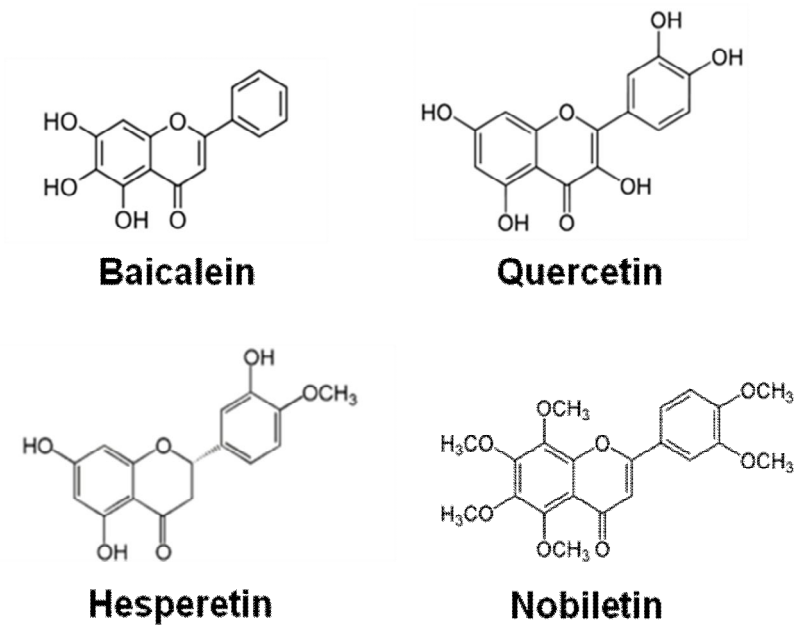

Figure. 14. Chemicals structure of flavonoids.

A

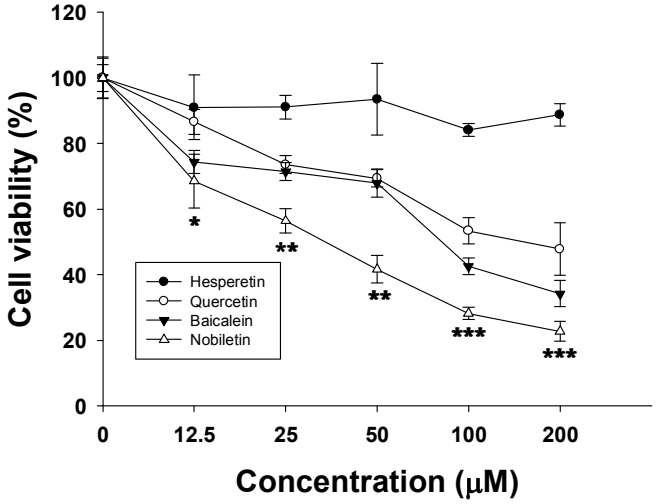

B

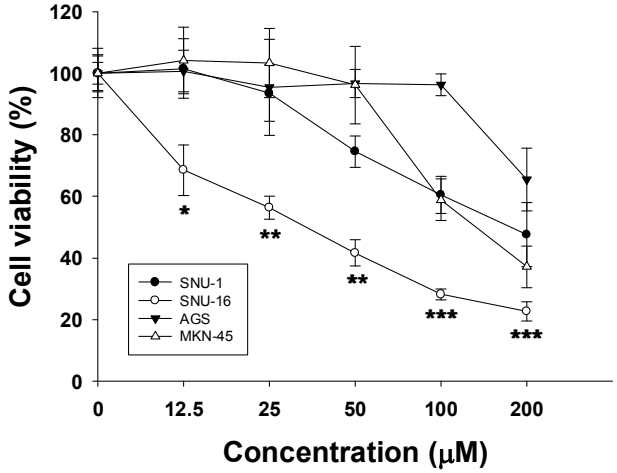

Figure. 15. Cell growth inhibition. Viability was determined on the basis of MTT reduction. A: SNU-16 human gastric cancer cells were treated with increasing doses of flavonoids for 48 h. B: Several stomach cancer cell lines were treated with nobiletin for 48 h. The assay (four replicates for each treatment) was repeated twice. Values are the mean ± SD of four independent experiments. **P*<0.05, ***P*<0.01, ****P*<0.001 compared to the control.

4.2. Effect of nobiletin on cell morphology, DNA laddering, and cell cycle distribution

Morphological changes such as cell shrinkage and condensation and fragmentation of chromatin are associated with apoptotic cell death. To evaluate the effect of nobiletin on proliferation and to characterize nobiletin-induced apoptosis, morphology and apoptosis in SNU-16 cells treated with various concentrations of nobiletin were examined by fluorescence microscopy after Hoechst 33342 staining. As shown in Figure. 16(A), after treatment with 25 and 50 μM nobiletin, SNU-16 cells showed obvious morphological changes, including condensed and fragmented chromatin and apoptotic bodies (arrows). Nobiletin induced DNA fragmentation in SNU-16 cells in a dose-dependent manner, as indicated by the appearance of DNA ladders in agarose gel electrophoresis analysis (Fig. 16B). Cell cycle control is the major regulatory mechanism of cell growth. In this study, signs of apoptosis were indicated by the accumulation of sub-G1 SNU-16 cells after nobiletin treatment. When applied for 24 h, nobiletin induced a concentration-dependent increase in the sub-G1 population from 4.48% (0 μM) to 33.42% (50 μM) (Table 8). Notably, in cells treated with a low concentration of nobiletin (12.5 μM), a significant increase occurred in the G1 population (from 58.42% to 72.24%). Taken together, these data suggest that nobiletin inhibits SNU-16 cell proliferation by inducing G1 cell cycle arrest at low concentrations and causing the accumulation of sub-G1 cells at high concentrations.

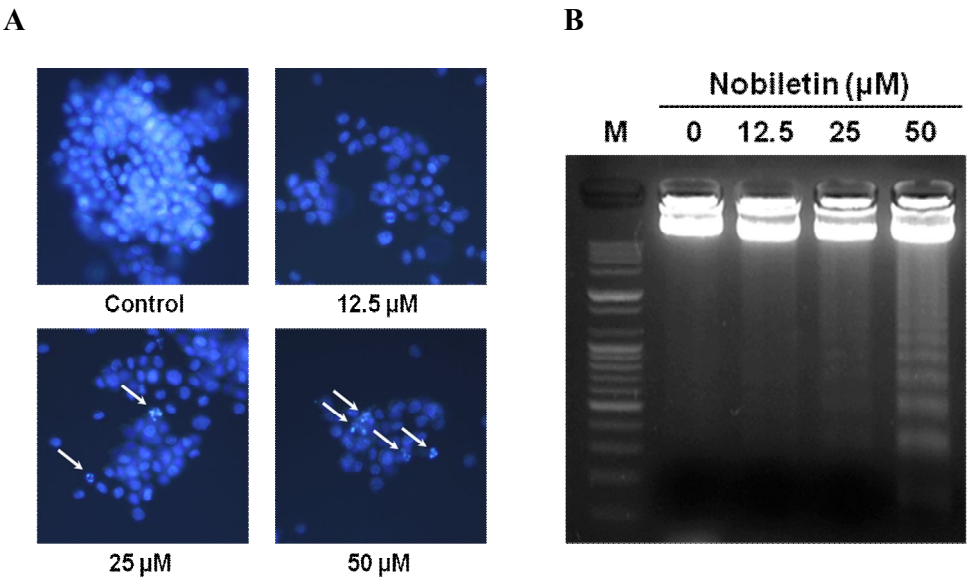

Figure. 16. Nuclear Hoechst 33342 staining and DNA fragmentation. A: Cells were treated with the indicated concentration of nobiletin (12.5-50 μM) for 24 h and then stained with Hoechst 33342. Stained cells were visualized under a fluorescence microscope. B: DNA fragmentation was analyzed by 1.8% agarose gel electrophoresis.

Table 8. The percentage of cell cycle phages in the nobiletin-treated SNU-16 cells for 24 hours.

Phase (%)	Nobiletin (μM)			
	0	12.5	25	50
Sub-G1	4.48±0.44	4.91±0.33	12.87±1.14	33.42±5.42
G1	58.42±0.24	74.24±0.77	69.47±0.28	44.13±3.03
S	18.49±0.69	8.76±0.88	6.30±0.63	10.53±0.91
G2/M	18.80±0.19	10.30±2.33	11.26±1.01	12.06±1.47

4.3. Effects of nobiletin on the expression of apoptosis-related proteins and p21

To determine the mechanism of nobiletin-induced apoptosis, the expression of anti- and pro-apoptotic proteins and activation of caspases following nobiletin treatment were examined by Western blotting. The protein level of the precursor of caspase-9 was reduced and proteolytically cleaved PARP levels were increased. A remarkable concentration-dependent decrease in the expression of Bcl-2 was noted, indicating that nobiletin induced apoptosis by shifting the Bax/Bcl-2 ratio in favor of apoptosis (Fig. 17). The expression of the cyclin-dependent kinase inhibitor $p21^{WAF1/CIP1}$ increased in cells treated with 12.5 μM nobiletin and then gradually decreased as the nobiletin concentration was increased. This result correlated with the increased number of G1 phase cells in cells treated with 12.5 μM nobiletin (Table 8). Because caspase-3 is one of the key executioners of apoptosis, we quantified its enzymatic activity using a commercially available kit. Nobiletin dose-dependently increased caspase-9, -3 activity (Fig.18). The present results indicate that nobiletin induced apoptosis in SNU-16 cells via the intrinsic pathway through activation of caspase-3 and caspase-9, and by increasing the Bax/Bcl-2 ratio.

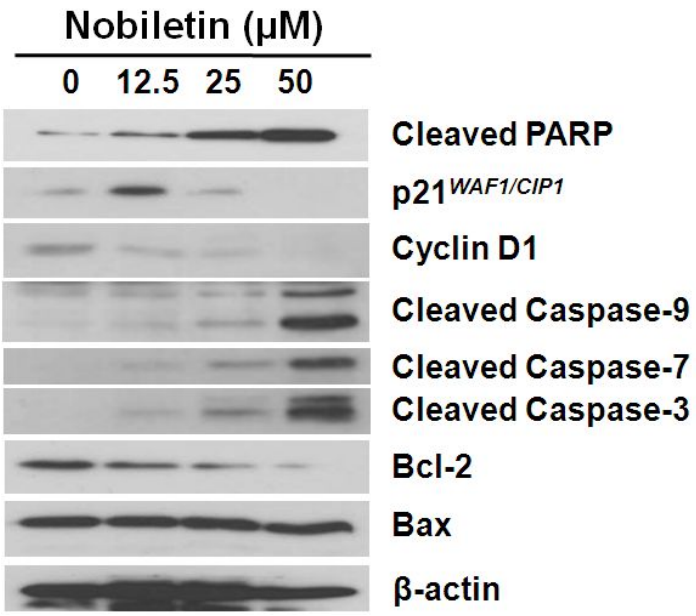

Figure. 17. Western blot analysis of apoptosis-related protein expression. Cells were lysed after incubation with different concentration of nobiletin (12.5–50 μM). After 24 h, cell lysates were subjected to Western blotting with antibodies against Cleaved PARP, $p21^{WAF1/CIP1}$, Cyclin D1, Cleaved Caspase-9, -7, -3, Bcl-2, Bax, and β-actin. Proteins were separated by SDS-PAGE and transferred onto PVDF membranes. The membranes were probed with the indicated primary antibodies. β-actin was used as an internal control.

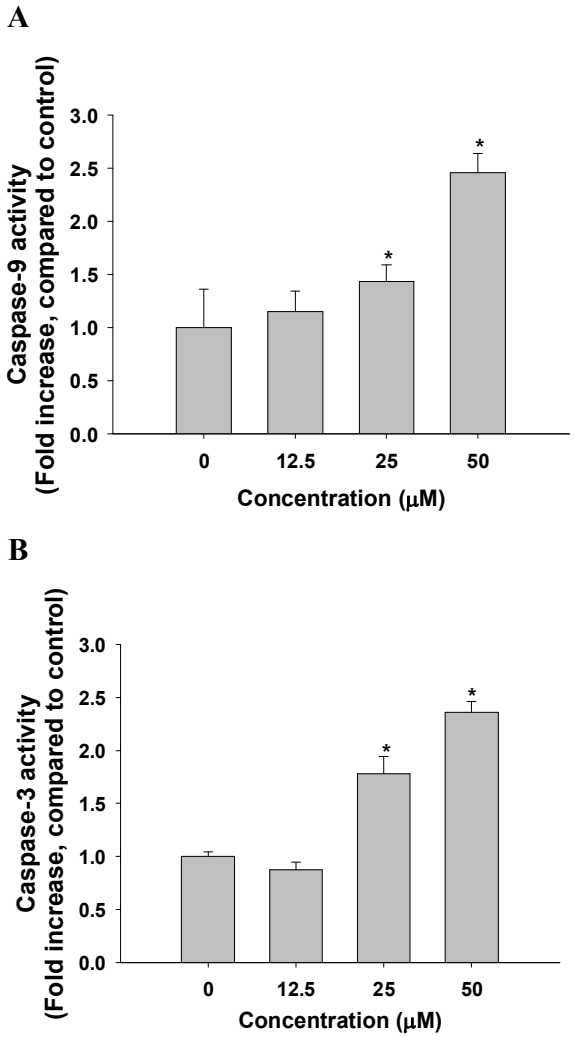

Figure. 18. Effect of nobiletin on Caspase-9, -3 activities in SNU-16 cells. Cell lysates prepared from cells that had been treated with nobiletin for 24 h were assayed for *in vitro* Caspase-9, -3 activity. The rate of cleavage of the caspase substrate LEHD-pNA, DEVD-pNA was determined by measuring the absorbance at 405 nm. The results are presented as the mean±SD. The experiments were performed in triplicate. **P*<0.05 compared to the control.

4. 4. Synergistic effects of nobiletin and 5-FU on SNU-16 cell growth

As whether nobiletin enhances or inhibits the activities of anticancer drugs is not clear, SNU-16 cells were incubated with a range of concentrations of nobiletin and 5-FU, and cell viability was then determined by MTT assay. When applied for 48 h, nobiletin and 5-FU reduced cell viability in a concentration-dependent manner (Fig. 19A). For combination treatment, the lowest effective dosage of each compound was combined with a range of doses of the other compound. In cells treated with 10 μM nobiletin plus 5-FU, cell growth inhibition increased by 19% as compared to cells treated with 5-FU alone; treatment of cells with 10 μM quercetin, baicalein, and hesperetin inhibited cell growth by 10%, 10%, and 8%, respectively (data not shown). The findings showed that 10 μM nobiletin and 10 μM 5-FU had a good synergistic effect (CI=0.377, Fig. B). For this reason, the combination of 10 μM nobiletin and 10 μM 5-FU was used in the following experiments to determine the possible mechanism of chemosensitization of cells to 5-FU by nobiletin.

A

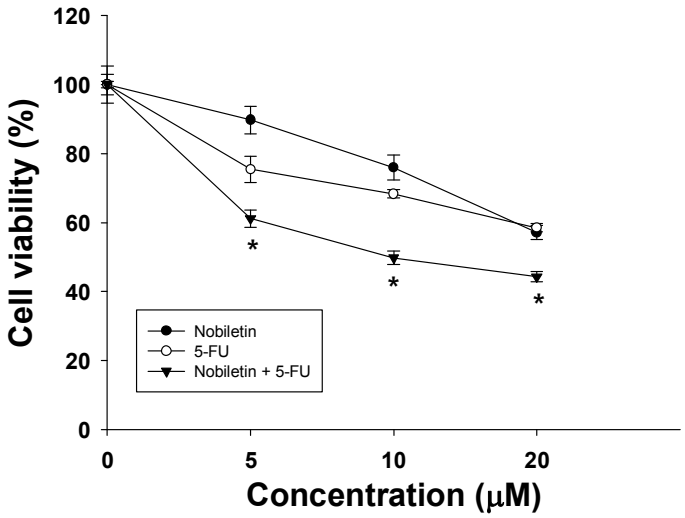

B

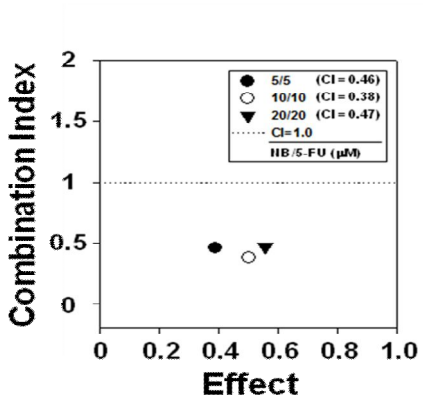

Figure. 19. Effect of nobiletin, 5-FU, and a combination of the two on the viability of SNU-16 cells. A: SNU-16 cells (5×10^4 cells/mL) were treated with nobiletin with or without 5-FU for 48 h. **P*<0.05 compared to treatment with 5-FU alone. B: Combination index (CI) for nobiletin plus 5-FU in SNU-16 human gastric cancer cells.

4. 5. p53-mutated SNU-16 cells respond to nobiletin and 5-FU via different pathways

To examine the mechanism by which nobiletin enhances the effects of 5-FU on SNU-16 cells, we first analyzed Hoechst 33342 staining and DNA fragmentation. The Hoechst 33342 staining and DNA laddering increased more significantly in SNU-16 cells treated with the combination of nobiletin and 5-FU than in cells treated with each compound alone (Fig. 20 A, and B). We also quantified the sub-G1 population, as a measure of apoptosis, after SNU-16 cells were exposed to 10 μM nobiletin and 5-FU for both 24 and 48 h. Combination treatment increased the proportion of sub-G1 phase cells at 24 and 48 h by 16.59% and 56.18%, respectively, as compared to cells treated with the same concentration of either compound alone (Table 9). The expression of proteolytically cleaved PARP, caspase-9, and caspase-3 did not differ significantly between cells exposed to combined treatment with nobiletin and 5-FU compared to those treated with 5-FU alone (Fig. 21). The expression of p53 protein and phosphorylation of p53 increased after treatment with 5-FU, but not with nobiletin, whereas the expression of $p21^{WAF1/CIP1}$ protein increased after treatment with nobiletin, but not with 5-FU. These data suggest that nobiletin and 5-FU inhibit human gastric cancer cell growth and induce apoptosis by modulating different pathways.

A

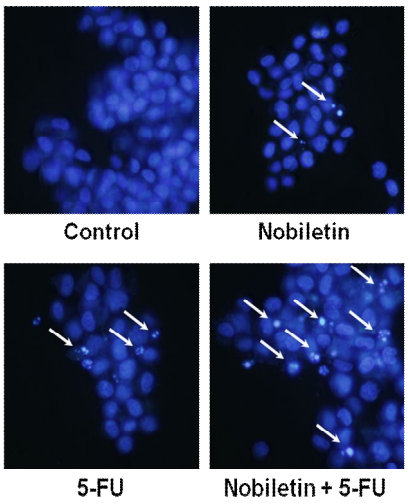

B

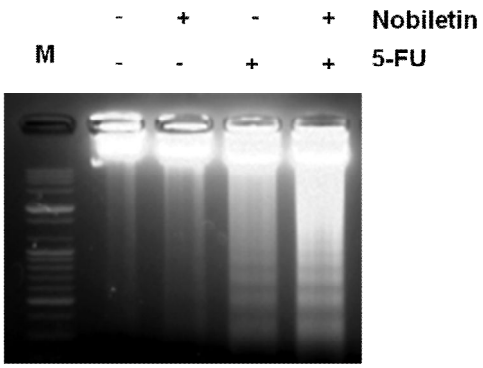

Figure. 20. Effect of co-treatment on nuclear Hoechst 33342 staining and DNA fragmentation. A: SNU-16 cells were treated with 10 μM nobiletin, 10 μM 5-FU, or a combination of the two for 48 h, and then stained with Hoechst 33342. Stained cells were observed under a fluorescence microscope. B: DNA fragmentation was analyzed by 1.8% agarose gel electrophoresis.

Table 9. The percentage of cell cycle phages in the nobiletin, fluorouracil and nobiletin plus fluorouracil -treated SNU-16 cells for 24 and 48 hours.

Phage (%)	Control (24 h)	N10 (24h)	F10 (24 h)	NF10 (24 h)	Control (48 h)	N10 (48 h)	F10 (48 h)	NF10 (48 h)
Sub-G1	6.99±3.41	6.71±0.95	11.76±6.06	16.59±5.34	4.77±1.52	7.39±3.25	41.42±10.15	56.18±7.03
G1	50.35±3.34	58.84±6.09	60.35±5.88	60.42±6.01	44.49±1.73	46.83±3.44	32.95±3.47	25.47±9.94
S	22.14±2.96	16.73±0.97	21.43±3.09	15.10±3.67	27.30±1.66	22.99±1.13	21.82±4.94	8.42±1.76
G2/M	21.09±2.60	18.21±4.84	7.36±0.91	8.34±2.22	24.01±4.95	23.31±3.11	4.46±3.01	5.54±0.96

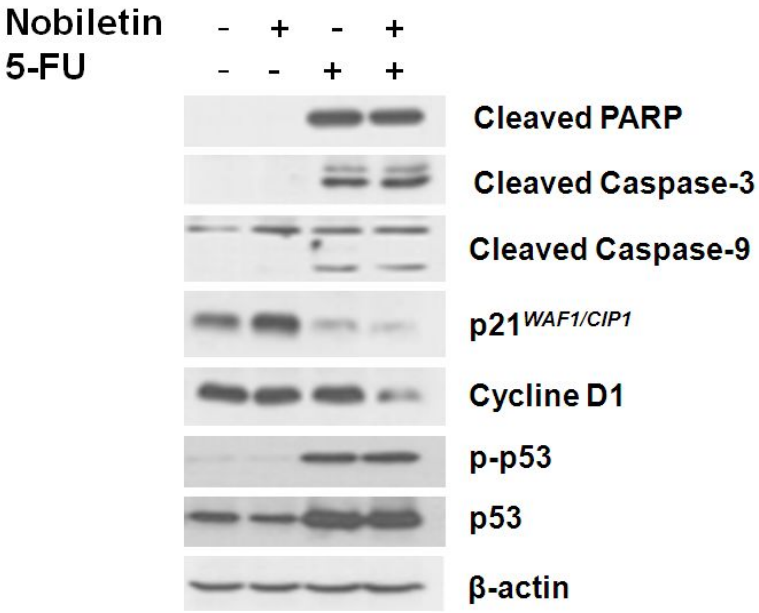

Figure. 21. Western blot analysis of protein expression in SNU-16 cells. After 48 h, cell lysates were subjected to western blotting with antibodies against Cleaved PARP, Cleaved Caspase-3, -9, $p21^{WAF1/CIP1}$, Cyclin D1, p-p53, p53, and β-actin. The proteins were separated by SDS-PAGE and transferred onto PVDF membranes. The membranes were probed with the indicated primary antibodies. β-actin was used as an internal control.

4.6. Nobiletin induce level of GRP78 protein in SNU-16 cells

Furthermore, we have also investigated that how to change of proetin expression level in the nobiletin-induced apoptosis of the SNU-16 cells. In order to identify the cellular effectors of the nobiletin, we applied a 2-D gel electrophoresis and PMF (Peptide Mass Fingerprinting) proteomic analysis approach. The quantitative and qualitative analyses were performed in twice and an expression change was considered significant if the intensity of corresponding spot differed reproducibly increased or decreased in relative volume between treated with nobiletin and without cells. In total 62 spots were indicated that different expression level of proteins compare to control and nobiletin-induced apoptosis cells (Fig 22. A, and B). We choose 20 spots and performed indentification of its proteins. 17 spots were successfully identified; rho GDP dissociation inhibitor 1, 78 kDa glucose-regulated protein, TXNDC5 and comm domain containing protein 9, eukaryotic translation initiation factor 4E, peroxiredoxin3, -6 and so on (Table 10).

A B

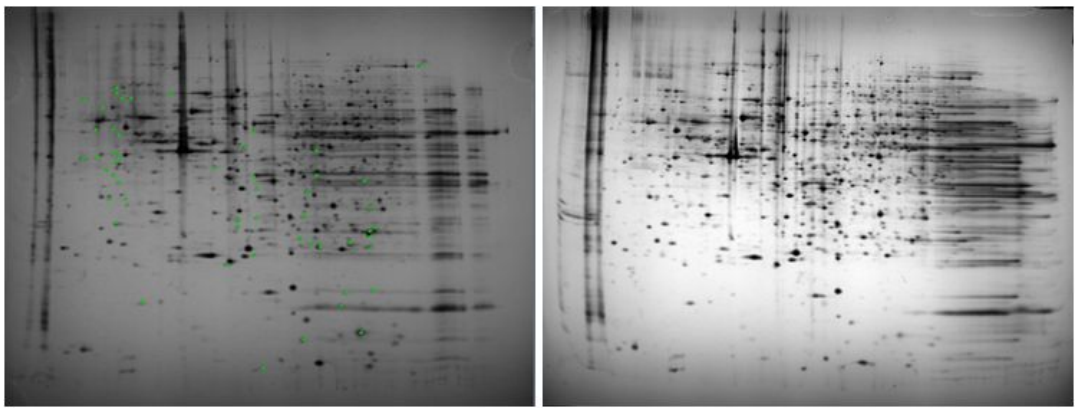

Figure. 22. Representative 2-DE maps of proteins of human gastric cancer SNU-16 cell line. (A: Control, B: treated-nobiletin 50 μM). The gels were silver stained. Solubilized proteins were focused on IPG strips (pH 4-10, 24 cm) and separated in SDS-polyacrylamide gradient gels (10–16%).

Table 10. Proteins identified from the 2-DE gels of human gastric cancer SNU-16 cell line by PMF.

	Identified protein	Score	Expect	Fold % vol.
1	spermine synthase	120	2.3e-07	3.34
2	Chain B, histocompatibility Antigen Hla-Dm	67	0.045	3.64
3	rho GDP-dissociation inhibitor 1 isoform a	135	7.4e-09	1.92
4	mitochondrial ATP synthase, H+ transporting F1 complex beta subunit	136	5.9e-09	3.22
5	78 kDa glucose-regulated protein	241	1.9e-19	6.44
6	TXNDC5 protein	233	1.2e-18	5.12
7	COMM domain-containing protein 9 isoform 2	91	0.00017	0.29
8	eukaryotic translation initiation factor 4E, isoform CRA_e	73	0.011	0.40
9	Chain A	183	1.2e-13	4.15
10	capping protein (actin filament) muscle Z-line, alpha 2, isoform CRA_a	93	0.00012	56.08
11	EF-hand calcium binding domain 6	85	0.00068	2.41
12	peroxiredoxin 3, isoform CRA_c	66	0.058	0.80
13	proteasome subunit beta type-3	71	0.017	0.69
14	Chain A, crystal structure of The Protein-Disulfide Isomerase Related Chaperone Erp29	66	0.055	0.60
15	fatty acid-binding protein, epidermal	64	0.083	0.58
16	peroxiredoxin-6	240	2.3e-19	0.60
17	proteasome subunit alpha type-6	133	1.2e-08	0.63

4.7. Nobiletin induce endoplasmic reticulum stress-mediated autophagy and apoptosis

To determine whether nobiletin has possible effects on ER, several ER-specific mediators were analysed. Initially, we focused on the expression levels of GRP78, using RT-PCR, and the results showed that activation occurred from 24 h of nobiletin treatment (Fig. 23 A). We next examined the expression level of GRP78 and caspase-4, using western blot, and the results indicated that nobiletin dose-dependently increase the GRP78 protein and activation of caspase-4 (Fig. 23 B).

We next investigated whether activation of ER stress is involved in the induction of autophagy in response to nobiletin treatment of cancer cells. Previous several data shown that THC-induced accumulation of de novo–synthesized ceramide, an event that occurs in the ER (Ogretmen and Hannun, 2004), leads to upregulation of the stress-regulated protein p8 and its ER stress–related downstream targets, ATF4, CHOP, and TRB3, to induce cancer cell death (Carracedo *et al.,* 2006). The result in Figure. 23 (B and C), showed that nobiletin increase expression level of GRP78 mRNA and protein in SNU-16. However, nobiletin could not increase level of GRP78 protein in AGS and SNU-1 cells. In addition, decrease the caspase-4, ER stress related protein, by nobiletin in SNU-16 cells. These results suggest that nobiletin-induced apoptosis with ER-stress in SNU-16 cells, not AGS and SNU-1 cells

A

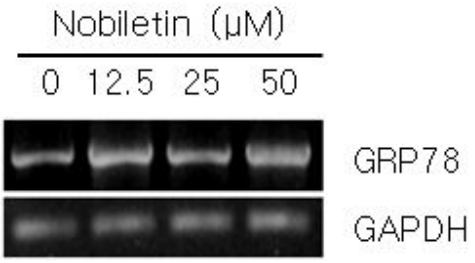

B

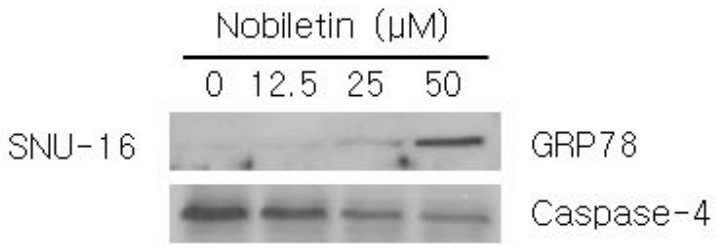

C

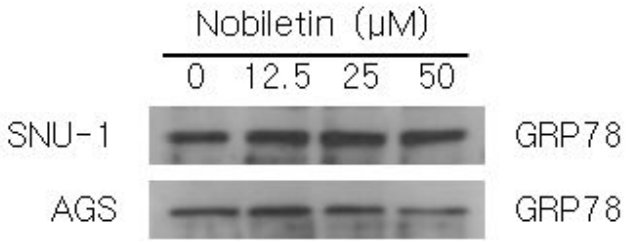

Figure. 23. RT-PCR and Western blot analysis of protein expression in gastric cancer cells. (A) Expression of GRP78 in SNU-16 cells after treatment of nobiletin was determined by RT-PCR. (B) After 24 h, cell lysates were subjected to western blotting with antibodies against GRP78 and caspase-4 in SNU-16 cells. (C) Western blotting with GRP78 antibody against in another gastric cancer cells, SNU-1 and AGS.

4.8. Nobiletin induced autophagy through the Akt/mTRO signaling pathway in SNU-16 cells

Recently, many research papers reported that ER stress can be the reason of autophagy (Ciechomska *et al*., 2012). In order to confirm whether ER-stress caused by nobiletin can induce autophagy or not, we performed western blot. The results of Akt/mTOR signaling in nobiletin-treated SNU-16 cells from western blot analysis are shown in Figure 24. The results indicated that nobiletin-treated SNU-16 cells led to the significant decrease of p-Akt and p-mTOR in nobiletin dose- and time-dependent manner (Fig. 24 A and B). Nobiletin also could increase the LC3B II, autophagy marker protein, compare to control in SNU-16 cells.

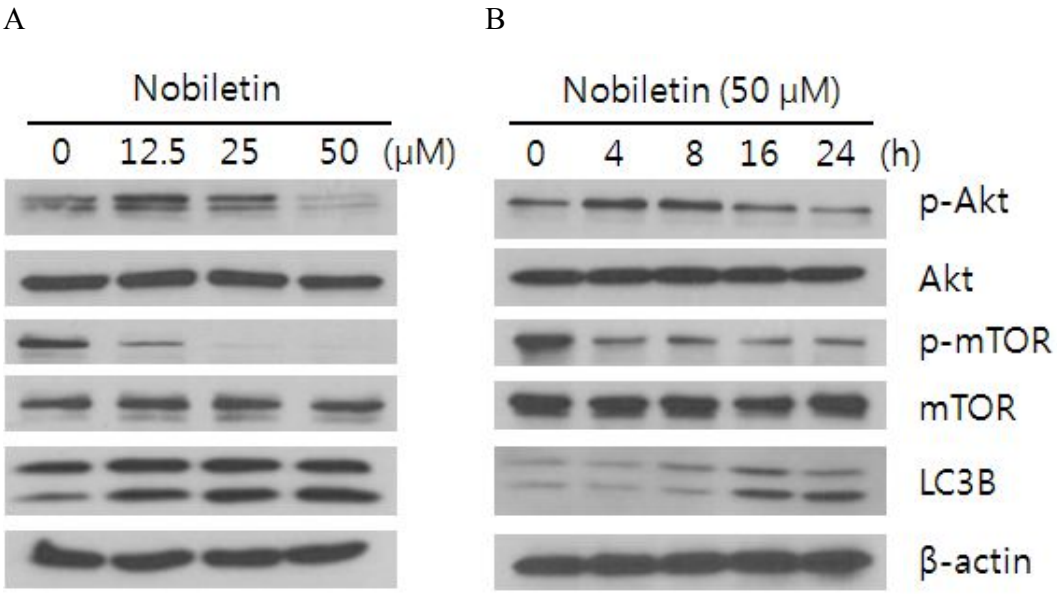

Figure. 24. Expression level of autophagy related proteins in SNU-1 cells. Cells were incubated with various concentration of nobiletin for 24 h (A) or 50 μM of nobiletin with time-dependent manner (B). Proteins were separated by SDS-PAGE in a 10-15% polyacrylamide gel, transferred to a PVDF membrane and immuno-reacted with autophagy antibodies.

4.9. Inhibition of autophagy enhances antiproliferative effects of nobiletin in SNU-16 cells

In addition, the role of autophagy in the nobiletin-mediated apoptosis was also investigated using autophagy inhibitor chloroquine. The cell proliferation after exposure of SNU-16 cells to 25 μM of nobiletin for 24 and 48 h was significantly reduced in the presence of chloroquine (Fig. 25 A). Western blotting result also indicated that nobiletin was increased of cleaved PARP in the presence of autophagy inhibitor, chloroquine (Fig. 25 B). We also examined the sub-G1 population after SNU-16 cells were treated to nobiletin and chloroquine for 24 h. Pre-treatment of chloroquine increased the proportion of sub-G1 phase rather than nobiletin 25 and 50 μM, 5.87% and 8.90%, respectively, as compared to cells treated with nobiletin alone (Table 11). Taken together, these results suggested that nobiletin induced ER stress-mediated apoptosis, and if inhibition of nobiletin-mediated autophagy sensitized these cancer cells death.

A

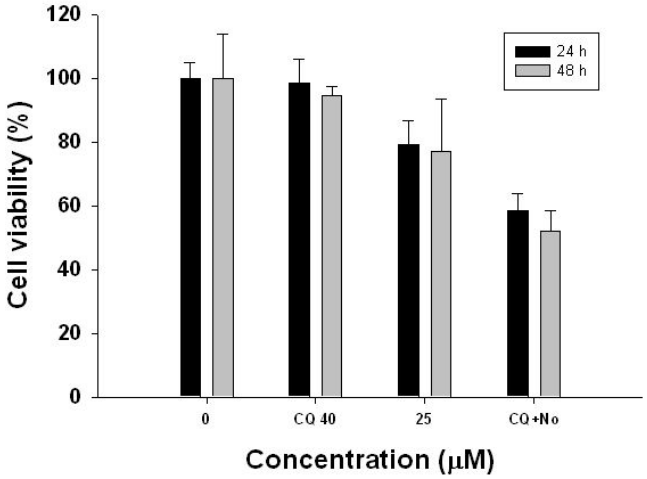

B

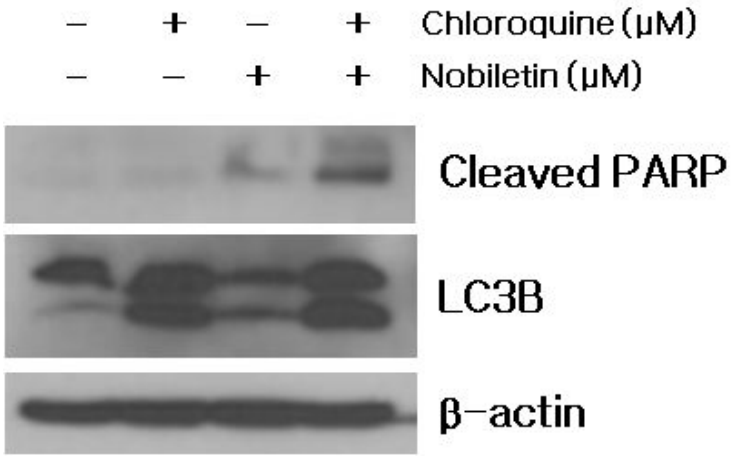

Figure. 25. Chloroquine inhibits autophagy and sensitizes SNU-16 cells to cytotoxic actions of nobiletin. (A) Cell viability was determined by MTT assay after treatment with different time (24 and 48 h) of nobiletin in the absence or presence of chloroquine (40 μM, pretreated for 2 h). (B) Western blot analysis of cleaved PARP expressions in cells treated with 25 μM nobiletin in the absence or presence of chloroquine (40 μM).

Table 11. Inhibition of autophagy enhance nobiletin-induced apoptosis

Phage (%) \ (μM)	Control	CQ 40	NO 25	CQ+ NO 25	NO 50	CQ+ NO 50
Sub-G1	7.93±4.67	9.61±2.84	17.16±2.91	**23.03±3.07**	30.91±7.40	**39.81±11.50**
G1	55.32±2.40	55.10±4.92	62.97±1.36	54.37±6.12	42.76±5.09	38.43±4.84
S	11.62±1.13	11.45±2.43	4.24±0.89	6.23±2.42	7.88±1.49	7.55±1.81
G2/M	25.47±5.33	24.17±2.74	15.79±3.32	16.62±3.60	18.76±2.25	14.55±5.68

5. DISCUSSION

Dietary phytochemicals have been shown to induce apoptosis through the modulation of different pathways contributing to decreased tumor malignance and chemoresistance (Ramos, 2008; Subapriya Rajamanickam, 2008). Nobiletin (5,6,7,8,3',4'-hexamethoxy), an effective component from citrus fruit, has been proved to inhibit some kinds of tumor cells proliferation (Tang, 2007) and tumor invasion (Kawabata, 2005; Lee, 2011) and to induce p53-mediated cell cycle arrest and apoptosis (Luo, 2008). Although it is quite clear that nobiletin may inhibit the growth of various cancers by inducing cancer cells towards the apoptosis or metastasis, there is no available information regarding the antitumor effects of nobiletin on human gastric cancer cells SNU-16 which is p53 mutant. Therefore, the present study was carried out to address the issue if nobiletin has antipoliferative effects or be able to induce apoptosis in human stomach cancer cells and to determine the first time that combination of nobiletin and 5-FU exerted their effects synergistically to reduce cell viability and the possible mechanism for its activity.

In this study, nobiletin induced apoptosis in p53 mutated SNU-16 cells, through the increase of sub-G1 phase, DNA fragmentation, an increase in the Bax/Bcl-2 ratio, the activation of caspase-9, -3, and the degradation of poly (ADP-ribose) polymerase (PARP) protein. $p21^{WAF1/CIP1}$ is a cyclin-dependent kinase inhibitor (CKI). The $p21^{WAF1/CIP1}$ protein binds to and inhibits the activity of cyclin-CDK2 or -CDK4 complexes, and thus functions as a regulator of cell cycle progression at G1 phase (Harper, 1993; Pan, 2002; Phromnoi, 2010). Our data also increase of $p21^{WAF1/CIP1}$ induced cell growth inhibition with accompany by arrest of G1 phage. These data suggest that nobiletin-induced apoptosis was caused by p53-independent activated $p21^{WAF1/CIP1}$ and caspase-9, -3 dependent cell death (Fig. 17)

Also, nobiletin has synergistic effect of combination with anticancer drug 5-fluorouracil (5-FU). Combination treatment was increased the growth inhibition of

cell viability, the formation of apoptotic body, DNA fragmentation and sub-G1 phase compared to those treated with alone. However, in western blot analysis, combination treatement could not detect more increase the apoptotic proteins compared to nobiletin and 5-FU alone. We hypothesized that, not only apoptosis but also another pathway was involved inhibition of cell proliferation by combination of nobiletin and 5-FU. In previous report, 5-FU induced cell cycle arrest by stimulating expression level of p53 and $p21^{WAF1/CIP1}$ (Lee, 2005; Seo, 2011), in this study, however 5-FU did not increase the level of $p21^{WAF1/CIP1}$ in SNU-16, mutated p53 cell. But we confirmed that nobiletin were acted without p53 through increased level of $p21^{WAF1/CIP1}$ and G1 phase arrest. So we hypothesis that combination treatment of nobiletin and 5-FU was increased the cell proliferation of cell cycle arrest accompained by apoptosis in the SNU-16 cells.

Therefore, we can speculate cellular responses to nobiletin and 5-FU occurred through different pathways. Then we performed 2-D gel electrophoresis for elucidate the underlying molecular mechanisms of nobiletin-mediated cellular effects in SNU-16 cells., 2-D-gel electrophoresis of SNU-16 cells induced with nobiletin showed that total, marked 17 spots were successfully identified, 9 proteins are identified as up-regulated and 8 as down-regulated. We assessed the peptide mass fingerprints (PMF) of 17 spots and compared them with the theoretical PMF of identified proteins. Among the 17 spots, we performed in nobiletin-treated SNU-16 cells focus on the GRP78 expression. GRP78 protein increase by nobiletin in SNU-16 cells, but not AGS and SNU-1, and determined the level of another ER stress-related proteins caspase-4 and the level of LC3II protein as an autophagy marker. Furthermore, when nobiletin-induced autophagy was blocked by chloroquine (late autophagy inhibitor) treatment, the sub-G1 phase and the level of cleaved PARP were increased. Chloroquine treatment also, decreased the cell proliferation by MTT assay. Therefore, autophagy induced by nobiletin has a role in cell survival. These results suggest that SNU-16 cells are more sensitive to nobiletin than another phytochemicals, and the

effect was associated with a high sensitivity to ER stress-mediated apoptosis and protective autophagy. In summary, nobiletin increases p53-mutated SNU-16 cell apoptosis by caspase-dependent through Akt/mTOR, and the inhibition of autophagy contributes to the inhibition of cell growth.

REFERENCE

Adams RP. Identification of essential oils by ion trap mass spectrometry. New York: Academic press. 1989.

Arts IC, Hollman PC. Polyphenols and disease risk in epidemiologic studies. Am J Clin Nutr, 2005, 81, 317S-325S.

Atti-Santos AC, Rossato M, Serafini LA, Cassel E, Moyna P. Extraction of essential oils from lime (Citrus latifolia Tanaka) by hydrodistillation and supercritical carbon dioxide. Braz Arch Bio Technol, 2005, 48, 155-160.

Baehrecke EH. Autophagy: dual roles in life and death. Nat Rev Mol Cell Biol, 2005, 6, 505-510.

Benavente-Garcia O, Castillo J. Update on uses and properties of Citrus flavonoids: New findings in anticancer, cardiovascular, and anti-inflammatory activity. Journal of Agricultural and Food Chemistry, 2008, 56, 6185-6205.

Benson AB 3rd: New approaches to the adjuvant therapy of colon cancer. Oncologist, 2006, 11, 973-980.

Bourne HR, Sanders DA, McCormick F. The GTPas superfamily: Conserved structure and molecular mechanism. Nature, 1991, 349, 117-27.

Carracedo A, Lorente M, Egia A, Blázquez C, García S, Giroux V, Malicet C, Villuendas R, Gironella M, González-Feria L, Piris MA, Iovanna JL, Guzmán M,

Velasco G. The stress-regulated protein p8 mediates cannabinoid-induced apoptosis of tumor cells. Cancer Cell, 2006, 9, 301-312.

Ciechomska IA, Gabrusiewicz K, Szczepankiewicz AA, Kaminska B. Endoplasmic reticulum stress triggers autophagy in malignant glioma cells undergoing. Oncogene, 2012, 10, 174.

Cho SK, Yang SO, Kim SH, Kim H, Ko JS, Riu KZ, Lee HY, Choi HK. Classification and prediction of free-radical scavenging activities of dangyuja (Citrus grandis Osbeck) fruit extracts using 1H NMR spectroscopy and multivariate statistical analysis. J Pharm Biomed Anal, 2009a, 49, 567-571.

Choi SY, Hwang JH, Ko HC, Park JG, Kim SJ. Nobiletin from citrus fruit peel inhibits the DNA-binding activity of NF-kappaB and ROS production in LPS-activated RAW 264.7 cells. J Ethnopharmacol, 2007, 113, 149-55.

Chou TC, Talalay P. Quantitative analysis of dose-effect relationships: the combined effects of multiple drugs or enzyme inhibitors. Adv Enzyme Regul, 1984, 2, 27-55.

Codogno P, Meijer AJ. Autophagy and signaling: their role in cell survival and cell death. Cell Death Differ, 2005, 12, 1509-1518.

Crowell PL. Prevention and therapy of cancer by dietary monoterpenes. In J Nutr, 1999, 129, 775-778.

Curini M, Cravotto G, Epifano F, Giannone G. Chemistry and biological activity of natural and synthetic prenyloxycoumarins. Curr Med Chem, 2006, 13, 199-222.

Ding WX, Ni HM, Gao W, Hou YF, Melan MA, Chen X, Stolz DB, Shao ZM, Yin XM. Differential effects of endoplasmic reticulum stress –induced autophagy on cell survival. J Biol Chem, 2007, 282, 4702-4710.

Elegbede JA, Elson CE, Qureshi A, Tanner MA, Gould MN. Inhibition of DMBA-induced mammary cancer by the monoterpene d-limonene. Carcinogenesis, 1984, 5, 661-664.

El-Shemy HA, Aboul-Enein AM, Aboul-Enein KM, Fujita K: Willow Leaves' Extracts Contain Anti-Tumor Agents Effective against Three Cell Types. PLoS ONE, 2007, 2, e178.

Fernandez J, Gharahdaghi F, Mische SM. Routine identification of proteins from sodium dodecyl sulfate-polyacrylamide gel electrophoresis (SDS-PAGE) gels or polyvinyl difluoride membranes using matrix assisted laser desorption/ionization-time of flight-mass spectrometry (MALDI-TOF-MS). Electrophoresis, 1998, 19, 1036-45.

Fuentes-Prior P, Salvesen GS. The protein structures that shape caspase activity, specificity, activation and inhibition. Biochem J, 2004, 384, 201-232.

Fujita E, Kouroku Y, Isoai A, Kumagai H, Misutani A, Matsuda C, Hayashi YK, Momoi T. Two endoplasmic reticulum-associated degradation (ERAD) systems for the novel variant of the mutant dysferlin: ubiquitin/proteosome ERAD(1) and autophagy/lysosome ERAD (II). Hum Mol Genet, 2007, 16, 618-629.

Haag JD, Lindstrom MJ, Gould MN. Limonene induced regression of mammary carcinomas. Cancer Res, 1992, 52, 4021-4026.

Hannay JB, Hogarth J. On the solubility of solids in gases. Proc R Soc Lond, 1879, A29, 324.

Hariya T. The possibility of regulating the function of adipose cells by odorants. Aroma Research, 2003, 13, 72-78.

Harper JW, Adami GR, Wei N, Keyomarsi K, Elledge SJ. The p21 Cdk-interacting protein Cip1 is a potent inhibitor of G1 cyclin-dependent kinases. Cell, 1993, 75, 805-816.

Haupt S, Berger M, Goldberg Z, Haupt Y. Apoptosis - the p53 network. J Cell Sci, 2003, 116, 4077-4085.

Huang WY, Cai YZ, Zhang Y. Natural phenolic compounds from medicinal herbs and dietary plants: potential use for cancer prevention. Nutrition and Cancer, 2009, 62, 1-20.

Jayarpakasha GK, Mandadi KK, Poulose SM, Jadegoud Y, Naganagowda GA, Patil BS. Novel triterpenoid from Citrus aurantium L. possesses chemopreventive properties against human colon cancer cells. Bioorganic and Medicinal Chemistry, 2008, 16, 5939-5951.

Jirtle RL, Haag JD, Ariazi EA, Gould MN. Increased mannose 6-phosphate/insulin-like growth factor II receptor and transforming growth factor beta 1 levels during monoterpene-induced regression of mammary tumors. Cancer Res, 1993, 53, 3849-3852.

Kaji I, Tatsuta M, Iishi H, Baba M, Inoue A, Kasugai H. Inhibition by D-limonene of experimental hepatocarcinogenesis in Sprague-Dawley rats does not involve P21RAS plasma membrane association. Int J Cancer, 2001, 93, 441-444.

Kamal GM, Anwar F, Hussain AI, Sarri N, Ashraf MY. Yield and chemical composition of Citrus essential oils as affected by drying pretreatment of peels. International Food Research Journal, 2011, 18, 1275-1282.

Kaufman RJ. Orchestrating the unfolded protein response in health and disease. J Clin Investig, 2002, 110, 1389-1398.

Kawabata K, Murakami A, Ohigashi H. Nobiletin, a citrus flavonoid, down-regulates matrix metalloproteinase-7 (matrilysin) expression in HT-29 human colorectal cancer cells. Biosci Biotechnol Biochem, 2005, 69, 307-314

Kim H, Moon JY, Mosaddik A, Cho SK. Induction of apoptosis in human cervical carcinoma HeLa cells by polymethoxylated flavone-rich Citrus grandis Osbeck (Dangyuja) leaf extract. Food Chem Toxicol, 2010, 48, 2435-2442

Kubo M, Matsuda H, Tomohiro N, Harima S. Historical and pharmalogical study of Citrus hassaku. Yakushigaku Zasshi (The Journal of Japanese History of Pharmacy), 2005, 40, 47-51.

Lee BJ, Chon KM, Kim YS, An WG, Roh HJ, Goh EK, Wang SG. Effects of cisplatin, 5-fluorouracil, and radiation on cell cycle regulation and apoptosis in the hypopharyngeal carcinoma cell line. Chemotherapy, 2005, 51, 103-110.

Lee YC, Cheng TH, Lee JS, Chen JH, Liao YC, Fong Y, Wu CH, Shih YW. Nobiletin,

a citrus flavonoid, suppresses invasion and migration involving FAK/PI3K/Akt and small GTPase signals in human gastric adenocarcinoma AGS cells. Mol Cell Biochem, 2011, 347, 103-115.

Leite M, Fassin J, Baziloni E, Almeida R, Mattei R, Leite J. Behavioral effects of essential oil of Citrus aurantium L. inhalation in rats. In Braz J Pharmacogn, 2008, 18, 661-666.

Leung WK, Wu MS, Kakugawa Y, Kim JJ, Yeoh KG, Goh KL, Wu KC, Wu DC, Sollano J, Kachintorn U, Gotoda T, Lin JT, You WC, Ng EK, Sung JJ. Screening for gastric cancer in Asia: current evidence and practice. Lancet Oncol, 2008, 9, 279-287.

Li S, Lambros T, Wang Z, Goodnow R, Ho CT. Efficient and scalable method in isolation of polymethoxyflavones from orange peel extract by supercritical fluid chromatography. J Chromatogr, B, 2007, 846, 291-297.

Lim HK, Yoo ES, Moon JY, Jeon YJ, Cho SK. Antioxidant activity of extracts from Dangyuja (Citrus grandis Osbeck) fruit produced in Jeju Island. Food Sci Biotechnol, 2006, 15, 312-316.

Lim HK, Moon JY, Kim H, Cho M, Cho SK. Induction of apoptosis in U937 human leukaemia cells by the hexane fraction of an extract of immature Citrus grandis Osbeck fruits. Food Chem, 2009, 114, 1245-1250.

Lota M, Serra D, Jacquemond C, Tomi F, Casanova J. Chemical Variability of Peel and Leaf Essential Oils of Sour Orange. In Flavour Fragr J, 2001, 16, 89-96.

Luo G, Guan X, Zhou L. Apoptotic effect of citrus fruit extract nobiletin on lung

cancer cell line A549 in vitro and in vivo. Cancer Biol Ther, 2008, 7, 966-973.

Luque de Castro MD, Valcarel M, Tena MT. Analytical Supercritical Fluid Extraction, Springer, Berlin, 1994.

Maiuri MC, Zalckvar E, Kimchi A, Kroemer G. Self-eating and selfkilling: crosstalk between autophagy and apoptosis. Nat Rev Mol Cell Biol, 2007, 8, 741-752

Manthey JA, Guthrie N. Antiproliferative activities of citrus flavonoids against six human cancer cell lines. J Agric Food Chem, 2002, 50, 5837-5843.

McHugh MA, Krukonis VJ. Supercritical Fluid Extraction, second ed., Butterworth-Heinemann, Boston, 1994.

McNamee D. d-Limonene trial in cancer. Lancet, 1993, 342, 801-805.

Meusser B, Hirsch C, Jarosch E, Sommer T. ERAD: the long road to destruction. Nat Cell Biol, 2005, 7, 766-772.

Modey WK, Mulholland DA, Raynor MW. Analytical Supercritical Fluid Extraction of Natural Products. Phytochem Anal, 1996, 7, 1.

Mohamed A, Emary G, Ali H. Influence of Some Citrus Essential Oils on Cell Viability, Glutathione-S-Transferase and Lipid Peroxidation in Ehrlich Ascites Carcinoma Cells. In Journal of American Science, 2010, 6, 820-826.

Mokbel MS, Hashinaga F. Evaluation of the antioxidant activity of extracts from buntan (Citrus grandis Osbeck) fruit tissues. Food Chem, 2006, 94, 529-534.

Moon JY, Kim H, Cho M, Chang WY, Kim CT, Cho SK. Induction of apoptosis in SNU-16 human gastric cancer cells by the chloroform fraction of extracts of Dangyuja (Citrus grandis) leaves. J Korean Soc Appl Biol Chem, 2009, 52, 168-175.

Morishima N, Nakanishi K, Takenouchi H, Shibata T, Yasuhiko Y. An endoplasmic reticulum stress-specific caspase cascade in apoptosis: cytochrome c-independent activation of caspase-9 by caspase-12. J Biol Chem, 2002, 277, 34287-34294.

Nakaizumi A, Baba M, Uehara H, Lishi H, Tatsuta M. d-limonene inhibits N-nitrosobis (2-oxopropyl) amine induced hamster pancreatic carcinogenesis. Cancer Lett, 1997, 117, 99-103.

Oakley BR, Kirsch DR, Morris NR. A simplified ultrasensitive silver stain for detecting proteins in polyacrylamide gels. Anal Biochem, 1980, 105, 361-363.

Ogata M, Hino S, Saito A, Morikawa K, Kondo S, Kanemoto S, Murakami T, Taniguchi M, Tanii I, Yoshinaga K, Shiosaka S, Hammarback JA, Urano F, Imaizumi K. Autophagy is activated for cell survival after endoplasmic reticulum stress. Mol Cell Biol, 2006, 26, 9220-9231.

Ogretmen B, Hannun YA. Biologically active sphingolipids in cancer pathogenesis and treatment. Nat Rev Cancer, 2004, 4, 604-616.

Ohtsu A. Chemotherapy for metastatic gastric cancer: past, present, and future. J Gastroenterol, 2008, 43, 256-264.

Oyadomari S, Mori M. Roles of CHOP/GADD153 in endoplasmic reticulum stress.

Cell Death Differ, 2004, 11, 381-389.

Pan MH, Chen WJ, Lin-Shiau SY, Ho CT, Lin JK. Tangeretin induces cell-cycle G1 arrest through inhibiting cyclin-dependent kinases 2 and 4 activities as well as elevating Cdk inhibitors P21 and P27 in human colorectal carcinoma cells. Carcinogenesis, 2002, 23, 1677-1684.

Park DJ, Lenz HJ. Determinants of chemosensitivity in gastric cancer. Curr Opin Pharmacol, 2006, 6, 337-344.

Patil Jaiprakash R, Jayaprakasha GK, Chidambara Murthy KN, Tichy SE, Chetti MB, Patil BS. Apoptosis-mediated proliferation inhibition of human colon cancer cells by volatile principles of Citrus aurantifolia. Food Chemistry, 2009, 114, 1351-1358.

Phromnoi K, Reuter S, Sung B, Limtrakul P, Aggarwal BB. A Dihydroxy-pentamethoxyflavone from Gardenia obtusifolia suppresses proliferation and promotes apoptosis of tumor cells through modulation of multiple cell signaling pathways. Anticancer Res, 2010, 30, 3599-3610.

Porta ED, Reverehon D, Barth DC. Mandarin and lime peel oil processing by supercritical CO_2 desorption; deterpenation and high molecular weight compound elimination. J Essent Oil Res, 1997, 9, 515-522.

Ranalli A, Contento S, Lucera L, Pavone G, Di Giacomo G, Aloisio L, Di Gregorio L, Mucci A, Kourtikakis I. Characterization of carrot root oil arising from supercritical fluid carbon dioxide extraction. J Agric Food Chem, 2004, 52, 4795-4801.

Ramos S. Cancer chemoprevention and chemotherapy: dietary polyphenols and

signalling pathways. Mol Nutr Food Res, 2008, 52, 507-526.

Rao RV, Castro-Obregon S, Frankowski H, Schuler M, Stoka V, del Rio G, Bredesen DE, Ellerby HM. Coupling endoplasmic reticulum stress to the cell death program. J Biol Chem, 2002, 277, 21836-21842.

Rein J, Cork C, Furton KG. Factors Governing the Analytical Supercritical Fluid Extraction and Chromatography of Polycyclic Aromatic Hydrocarbons. J Chromatogr, 1991, 545, 149-160.

Schro¨der M, Kaufman RJ. ER stress and the unfolded protein response. Mutat Res, 2005, 569, 29-63.

Seo JS, Kim TG, Hong YS, Chen JY, Lee SK. Contribution of Epstein-Barr Virus Infection to Chemoresistance of Gastric Carcinoma Cells to 5-Fluorouracil. Arch Pharm, 2011, 34, 635-643.

Siddique S, Shafique M, Parveen Z, Khan S, Khanum R. Volatile Components, Antioxidant and Antimicrobial Activity of Citrus Aurantiumvar Bitter Orange Peel Oil. InPharmacologyonline, 2011, 2, 499-507.

Smith RM. Supercritical Fluid Chromatography. The Royal Society of Chemistry, London, 1988.

Sun XM, MacFarlane M, Zhuang J, Wolf BB, Green DR, Cohen GM. Distinct caspase cascades are initiated in receptor-mediated and chemical-induced apoptosis. J Biol Chem, 1999, 274, 5053-5060.

Subapriya Rajamanickam RA. Natural products and colon cancer: current status and future prospects. Drug Dev Res, 2008, 69, 460-471.

Tang M, Ogawa K, Asamoto M, Hokaiwado N, Seeni A, Suzuki S, Takahashi S, Tanaka T, Ichikawa K, Shirai T. Protective effects of citrus nobiletin and auraptene in transgenic rats developing adenocarcinoma of the prostate (TRAP) and human prostate carcinoma cells. Cancer Sci, 2007, 98, 471-477.

Teckman JH, Perlmutter DH. Retention of mutant alpha(1)-antitrypsin Z in endoplasmic reticulum is associated with an autophagic response. Am J Physiol Gastrointest Liver Physiol, 2000, 279, 961-974.

Tsai HL, Chang SK, Chang SJ. Antioxidant content and free radical scavenging ability of fresh red pummelo [Citrus grandis (L.) Osbeck] juice and freeze-dried products. J Agric Food Chem, 2007, 55, 2867-2572.

Ulukaya E, Acilan C, Yilmaz Y. Apoptosis: why and how does it occur in biology? Cell Biochem Funct, 2011, 29, 468-480

Vigushin DM, Poon GK, Boddy A, English J, Halbert GW, Pagonis C, Jarman M, Coombes RC. Phase I and pharmacokinetic study of d-limonene in patients with advanced cancer. Cancer Research Campaign Phase I/II Clinical Trials Committee. Cancer Chemother Pharmacol, 1998, 42, 111-7.

Wagner AD, Grothe W, Haerting J, Kleber G, Grothey A, Fleig WE. Chemotherapy in advanced gastric cancer: a systematic review and meta-analysis based on aggregate data. J Clin Oncol, 2006, 24, 2903-2909.

Yorimitsu T, Nair U, Yang Z, Klionsky DJ. Endoplasmic reticulum stress triggers autophagy. J Biol Chem, 2006, 281, 30299-30304.

Youle RJ, Strasser A, The BCL-2 protein family: opposing activities that mediate cell death. Nat Rev Mol Cell Biol, 2008, 9, 47-59.

List of Publications

Hee-Kyung Lim, **Jeong Yong Moon**, Hana Kim, Moonjae Cho, Somi Kim Cho. Induction of apoptosis in U937 human leukaemia cells by the hexane fraction of an extract of immature Citrus grandis Osbeck fruits. Food Chemistry (2009)

Jeong Yong Moon, Hana Kim, Moonjae Cho, Weon Young Chang, Cheong-Tae Kim, and Somi Kim Cho. Induction of Apoptosis in SNU-16 Human Gastric Cancer Cells by the Chloroform Fraction of an Extract of Dangyuja (Citrus grandis) Leaves. JKSABC (2009)

Hana Kim, **Jeong Yong Moon**,Hyeonji Kim, Dong-Sun Lee, Moonjae Cho, Hyung-Kyoon Choi, Young Suk Kim, Ashik Mosaddik, Somi Kim Cho. Antioxidant and antiproliferative activities of mango (Mangifera indica L.) flesh and peel. Food Chemistry (2010)

Hana Kim, **Jeong Yong Moon**, Ashik Mosaddik, Somi Kim Cho. Induction of apoptosis in human cervical carcinoma HeLa cells by polymethoxylated flavone-rich Citrus grandis Osbeck(Dangyuja) leaf extract. Food and Chemical Toxicology (2010)

HyeonJi Kim, Hyung-Kyoon Choi, **Jeong Yong Moon**, Young Suk Kim, Ashik Mosaddik, Somi Kim Cho. Comparative Antioxidant and Antiproliferative Activities of Red and White Pitayas and Their Correlation with Flavonoid and Polyphenol Content. Journal of Food Science (2010)

Jeong Yong Moon, Ashik Mosaddik, Hana Kim, Moonjae Cho, Hyung-Kyoon Choi, Young Suk Kim, Somi Kim Cho. The chloroform fraction of guava (Psidium. cattleianum sabine) leaf extract inhibits human gastric cancer cell proliferation via induction of apoptosis. Food Chemistry (2011)

Neung Jae Jun, Ashik Mosaddik, **Jeong Yong Moon**, Ki-Chang Jang, Dong-Sun Lee, Kwang Seok Ahn and Somi K. Cho. Cytotoxic activity of β-caryophyllene oxide isolated from Jeju Guava (Psidium cattleianum Sabine) Leaf. Records of Natural Products (2011)

Trang Thi Mai, **Jeong Yong Moon**, YeonWoo Song, Pham Quoc Viet, Pham Van Phuc, Jung Min Lee, Tae-Hoo Yi, Moonjae Cho, Somi Kim Cho. Ginsenoside F2 induces apoptosis accompanied by protective autophagy in breast cancer stem cells. Cancer Letters (2012)

Rajendra Gyawali, **Jeong Yong Moon**, Deok Hyeon Jeon, Hyeonji Kim, Yeon Woo Song, Ho Bong Hyun, So Young Moon, Tae Hwan Kang, Keun Sik Moon, Somi Kim Cho. Chemical composition and antiproliferative activity of supercritical CO_2 extracts from citrus fruits. Food Science and Technology Research (2012)

Rajendra Gyawali, Deok Hyeon Jeon, **Jeong Yong M**oon, Hyeon Ji Kim, Yeon Woo Song, Ho Bong Hyun, So Young Moon, Tae Hwan Kang, Keun Sik Moon, Somi Kim Cho. Chemical composition and antiproliferative activity of Citrus hassaku and Citrus iyo fruits. Czech journal of Food Sciences (2012)

Karthikeyan Krishnamoorthy, **Jeong Yong Moon,** Ho Bong Hyun, Somi Kim Cho and Sang-Jae Kim. Mechanistic Investigation on the Toxicity of MgO Nanoparticles toward Cancer Cells. Journal of Materials Chemistry (2012)

Jeong Yong Moon, Moonjae Cho, Kwang Seok Ahn, Somi Kim Cho. Nobiletin Induces Apoptosis and Potentiates the Effects of the Anticancer Drug 5-Fluorouracil in p53-Mutated SNU-16 Human Gastric Cancer Cells. Nutrion and Cancer (2013)

감사의 글

어느덧 이렇게 시간이 지나 박사과정을 졸업한다고 하니 그 동안의 세월동안 좀 더 열심히 하지 못한 점에 무척이나 아쉬운 마음이 듭니다. 매년 추운 겨울날이 오면 석사 졸업때가 생각나 새해마다 좀 더 열심히 하겠다는 목표를 세우지만 그 목표에는 제가 항상 미치지 못하였던 것 같습니다. 하지만 그런 저를 이렇게 끝까지 믿고 이끌어 주신 김소미 교수님의 은혜에 깊은 감사 드립니다. 그리고 저의 부족한 연구이지만 맡아서 심사를 해주신 류기중 교수님, 조문제 교수님, 이동선 교수님, 그리고 멀리서 찾아와주신 최형균 교수님께도 깊은 감사를 드립니다.

또한 제가 학부때부터 학문의 길에 들어선 후 저에게 많은 지도와 가르침을 주신 영미누나, 희경누나, 길남이형 외 많은 선생님들께 깊은 감사 드리며, 또한 항상 실험실에서 저를 도와주고 멀리서라도 응원해준 능재, 진영, 윤정, 하나, 정순, 현지, 덕현, 연우, 호봉이에게도 고맙다는 말을 전하고 싶습니다.

그리고 마지막으로 항상 옆에서 부족한 저를 응원해주고 지지해준 저의 아내와 아이들에게 고맙고 사랑한다는 말 전하고 싶고, 끝까지 저를 믿어주는 어머니와 동생, 그리고 지금은 하늘 나라에서 흐뭇한 웃음을 짓고 계실 아버지에게 이 영광을 바칩니다.

감사합니다.